JCI insight

Dual peroxisome-proliferator-activated-receptor-α/γ activation inhibits SIRT1-PGC1α axis and causes cardiac dysfunction

Charikleia Kalliora, Ioannis D. Kyriazis, Shin-ichi Oka, Melissa J. Lieu, Yujia Yue, Estela Area-Gomez, Christine J. Pol, Ying Tian, Wataru Mizushima, Adave Chin, Diego Scerbo, P. Christian Schulze, Mete Civelek, Junichi Sadoshima, Muniswamy Madesh, Ira J. Goldberg, Konstantinos Drosatos

JCI Insight. 2019. https://doi.org/10.1172/jci.insight.129556.

Research In-Press Preview Metabolism

Graphical abstract

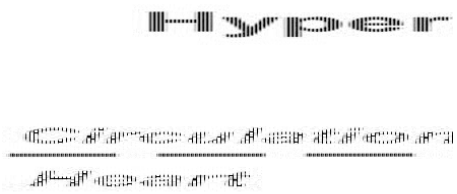

Dual Peroxisome-Proliferator-Activated-Receptor-α/γ activation inhibits SIRT1-PGC1α axis and causes cardiac dysfunction

Brief Summary: Tesaglitazar causes cardiac dysfunction via SIRT1 and PGC1α inhibition

Charikleia Kalliora[1,2 #], Ioannis D. Kyriazis[1, #], Shin-ichi Oka[3], Melissa J. Lieu[1], Yujia Yue[1], Estela Area-Gomez[4], Christine J. Pol[1], Ying Tian[1], Wataru Mizushima[3], Adave Chin[3], Diego Scerbo[5, 6], P. Christian Schulze[7], Mete Civelek[8], Junichi Sadoshima[3], Muniswamy Madesh[1], Ira J. Goldberg[6], Konstantinos Drosatos[1,*]

Affiliations: [1]Lewis Katz School of Medicine at Temple University, Center for Translational Medicine, Department of Pharmacology, 3500 N. Broad Street, Philadelphia, 19140, PA, USA. [2]Faculty of Medicine, University of Crete, Voutes, Greece. [3]Department of Cell Biology and Molecular Medicine, Cardiovascular Research Institute, Rutgers-New Jersey Medical School, Newark, 07103, NJ, USA. [4]Department of Neurology, Columbia University Medical Center New York, 10032, NY, USA. [5]Division of Preventive Medicine and Nutrition, Columbia University, New York, 10032, NY, USA. [6]NYU-Langone School of Medicine, Division of Endocrinology, Diabetes & Metabolism, 522 First Avenue, New York, 10016, USA. [7]Department of Internal Medicine I, Division of Cardiology, Angiology, Intensive Medical Care and Pneumology, University Hospital Jena, Erlanger Allee 101, 07747, Jena, Germany. [8]Department of Biomedical Engineering, Center for Public Health Genomics, University of Virginia, Charlottesville, 22908, VA, USA.

#Equal contribution

*To whom correspondence should be addressed: Konstantinos Drosatos, Metabolic Biology Laboratory, Temple University School of Medicine, Center for Translational Medicine, Department of Pharmacology, 3500 N. Broad Street, Philadelphia, 19140, USA; Tel: +1-215-707-1421, Fax: +1-215-707-9890; email: drosatos@temple.edu

ABSTRACT

Dual peroxisome proliferator-activated receptor (PPAR)α/γ agonists that were developed to target hyperlipidemia and hyperglycemia in type 2 diabetes patients, caused cardiac dysfunction or other adverse effects. We studied the mechanisms that underlie the cardiotoxic effects of a dual PPARα/γ agonist, tesaglitazar, in wild type and diabetic (leptin receptor deficient - *db/db*) mice. Mice treated with tesaglitazar-containing chow or high fat diet developed cardiac dysfunction despite lower plasma triglycerides and glucose levels. Expression of cardiac peroxisome proliferator-activated receptor gamma coactivator 1-alpha (PGC1α), which promotes mitochondrial biogenesis, had the most profound reduction among various fatty acid metabolism genes. Furthermore, we observed increased acetylation of PGC1α, which suggests PGC1α inhibition and lowered sirtuin 1 (SIRT1) expression. This change was associated with lower mitochondrial abundance. Combined pharmacological activation of PPARα and PPARγ in C57BL/6 mice reproduced the reduction of PGC1α expression and mitochondrial abundance. Resveratrol-mediated SIRT1 activation attenuated tesaglitazar-induced cardiac dysfunction and corrected myocardial mitochondrial respiration in C57BL/6 and diabetic mice but not in cardiomyocyte-specific *Sirt1*$^{-/-}$ mice. Our data shows that drugs, which activate both PPARα and PPARγ lead to cardiac dysfunction associated with PGC1α suppression and lower mitochondrial abundance likely due to competition between these two transcription factors.

INTRODUCTION

Aside from improvement in hyperglycemia, various new therapies for treatment of type 2 diabetes focus on the impact of the new drugs on cardiovascular disease. Agonists of peroxisome proliferator-activated receptor (PPAR)α and PPARγ have been developed for the treatment of hyperlipidemia and hyperglycemia, respectively, based on their effects in reducing circulating triglyceride levels and promoting insulin sensitization.

PPARs belong to the nuclear receptors super-family and promote fatty acid (FA) metabolism. PPARα ligands, such as fibrates, lower plasma triglyceride levels and increase high-density lipoprotein (HDL)-cholesterol levels (1). Thiazolidinediones are PPARγ ligands and act as insulin sensitizers that lower plasma glucose (2). However, PPARγ agonists have toxicity and can produce heart failure either due to direct actions on the heart or due to increased salt and water retention (3). Dual-PPARα/γ agonists (glitazars) were developed to combine the beneficial effects of PPARα and PPARγ agonism. Although these dual-agonists improve metabolic parameters (4), some of them, such as tesaglitazar (5) and muraglitazar (6) were abandoned when clinical trials showed either increased risk for cardiovascular events or other adverse effects, such as increased peripheral edema and creatine phosphokinase via mechanisms that remain unknown.

PPARs are central regulators of cardiac FA metabolism (7). Cardiac PPARα induces the expression of genes that orchestrate FA oxidation (FAO) and uptake (8). Greater FAO leads indirectly to lower cardiac glucose utilization (9). PPARγ can also promote cardiac FAO (10, 11), when PPARα expression is reduced (12) or ablated (11). Thus, both PPARα and PPARγ can orchestrate the cardiac FAO-related gene expression program. Because different PPAR isoforms can activate the same FA metabolism-related genes, dominance of one PPAR isoform over the other in controlling FA metabolism in a tissue depends on the abundance of the respective isoform, as well as on the availability of endogenous isoform-specific ligands. FAO accounts for 70% of the ATP that is produced in the heart (13). Thus, it is surprising that combined activation of two positive regulators of cardiac FAO, PPARα and PPARγ, causes cardiac dysfunction.

Peroxisome proliferator-activated receptor gamma coactivator 1-alpha (PGC1α) is encoded by the *Ppargc1a* gene. It is the common transcriptional coactivator of PPARα and PPARγ and regulates cardiac FAO, mitochondrial biogenesis, and respiration (14). PGC1α activation is controlled through reversible lysine side chain hyperacetylation that is attenuated by the enzymatic activity of the deacetylase sirtuin1 (SIRT1) (15). SIRTs are class III histone deacetylases activated by nicotinamide adenine dinucleotide (NAD^+). Thus, they act as metabolic sensors of fluctuations in the NAD^+/NADH ratio (16).

In this study, we investigated the effect of combined PPARα/γ activation on PGC1α expression and activation. Subsequently, we assessed whether the inhibitory effect of dual PPARα/γ activation on PGC1α activity is driven by downregulation of SIRT1. Our data show that cardiac dysfunction caused by an antidiabetic dual-PPARα/γ agonist, tesaglitazar, is associated with reduced PGC1α expression and activation (17-19). These effects are associated with competition between PPARα and PPARγ for regulation of *Ppargc1a* gene expression, as well as by decreased cardiac SIRT1 expression. Activation of SIRT1 with resveratrol attenuated tesaglitazar-mediated cardiac dysfunction in C57BL/6 wild type and in diabetic *db/db* (leptin receptor deficient) mice, but not in mice with cardiomyocyte-specific ablation of SIRT1. Our data elucidate the mechanism that underlies dual PPARα/γ activation cardiotoxicity and identify a new pharmacologic approach to prevent these side effects.

RESULTS

Tesaglitazar causes cardiac dysfunction

Six weeks old C57BL/6 male mice were fed on standard diet (chow) supplemented with tesaglitazar for 6 weeks. Tesaglitazar feeding did not alter plasma triglycerides or glucose levels (Figures 1A, 1B) and neither did it affect weight gain rate and food consumption compared to their respective controls (Figures S1A-S1B). On the other hand, 2D-echocardiography revealed that mice fed with tesaglitasar developed cardiac dysfunction (Figures 1C, D). Specifically, tesaglitazar reduced FS% by ~20% and increased left ventricular internal diameter during systole (LVIDs) by 30%, compared to chow-fed mice (Figure 1D and Table S1).

Tesaglitazar-mediated cardiac dysfunction is associated with lower PGC1α protein levels

Because tesaglitazar is a dual agonist for both PPARα and PPARγ, we examined expression of cardiac FAO-genes in mice treated with tesaglitazar. The expression of *Ppargc1a*, which encodes for the common transcriptional co-activator of PPARs (20) and promotes mitochondrial biogenesis, showed a strong trend (p=0.104) for reduction (20%) at the mRNA level (Figure 1E) and clear reduction (~45%) at the protein level (Figure 1F). Among several fatty acid (FA) metabolism related genes, *Ppard* expression was increased by 2.6-fold and uncoupling protein 3 (*Ucp3*) expression had a strong trend of increase (87%; Figure 1G). In contrast to these changes, cardiac PPARα and PPARγ protein levels were not significantly altered in tesaglitazar-treated mice (Figures S1C, D).

PPARα activation compromised PPARγ-mediated induction of PGC1α

To test whether the effect of tesaglitazar in PGC1α levels relies on combined activation of PPARα and PPARγ, we tested whether individual PPARα and PPARγ activation by their respective ligands has a similar effect. First, we performed dose titration experiments to identify the minimum dose of rosiglitazone (PPARγ agonist) that increases cardiac *Ppargc1a* expression levels and the maximum dose of WY-14643 (PPARα agonist) that does not affect it. Specifically,

we administered a series of doses of rosiglitazone or WY-14643 (25mg/kg body weight, 12.5mg/kg body weight, 6.25mg/kg body weight, 3.125mg/kg body weight) via intraperitoneal (i.p.) injections in C57BL/6 mice. This experiment showed that 25mg/kg body weight was the lowest dose of rosiglitazone that induced cardiac *Ppargc1a* expression (Figure 2A) and 12.5mg/kg body weight was the highest dose of WY-14643 that did not (Figure 2A). C57BL/6 mice were then injected with combination of 25mg/kg body weight rosiglitazone and 12.5mg/kg body weight WY-14643. The combined treatment prevented rosiglitazone-mediated upregulation of cardiac *Ppargc1a* gene expression (Figure 2A). Accordingly, combined administration of rosiglitazone and WY-14643 prevented PPARγ-mediated upregulation of the expression of lipid uptake-related genes, such as cluster of differentiation 36 (*Cd36*) and *Lpl* (Figure 2B). Rosiglitazone also increased *CPT1B* (2.3-fold), *ACOX1* (2.5-fold) mRNA levels but combined injection of both PPARα and PPARγ agonists in C57BL/6 mice blocked the effects of rosiglitazone (Figure 2C). Conversely, PPARα and PPARγ did not seem to compete for regulation of other genes. Specifically, treatment of C57BL/6 mice with WY-14643 did not prevent rosiglitazone-mediated trend of increase of *Acadl* (~25-fold) gene expression (Figure 2C)**.** Cardiac *Ucp3* gene expression was increased (3.2-fold) by WY-14643 and retained the same levels in mice treated with the combination (Figure 2C)**.** On the other hand, both individual agonist treatments, as well as combined administration, increased the expression of *Angptl4* with rosiglitazone being the major inducer (single treatment: 35-fold and combined treatment: strong trend of 25-fold increase), compared to WY-14643 single treatment (2.5-fold) (Figure 2B). Thus, although combined-PPARα/γ activation led to greater expression of some FAO-related genes, the expression of *Ppargc1a* and some other downstream PPAR targets was not increased.

Combined PPARα/γ activation decreased cardiac mitochondrial abundance and respiration

PGC1α promotes mitochondrial biogenesis (14) by controlling the expression of mitochondrial transcription factor A (mtTFA, encoded by *Tfam* gene) (21). Given that combined administration of single PPARα and PPARγ agonists prevented rosiglitazone-mediated

upregulation of PGC1α, and treatment with the dual-PPARα/γ agonist, tesaglitazar, had an inhibitory effect on cardiac PGC1α levels, we tested whether combined PPARα and PPARγ activation affects mitochondrial abundance and function. Cardiac *TFAM* mRNA levels were increased (2-fold) in rosiglitazone-treated C57BL/6 mice, but combined treatment with rosiglitazone and WY-14643 prevented this increase (Figure 3A). Conversely, hearts from mice treated with combination of rosiglitazone and WY-14643 exhibited reduced mitochondrial DNA (mtDNA) to nuclear DNA (nuDNA) ratio (-31%; Figure 3B), demonstrating that combined activation of PPARα and PPARγ, prevents rosiglitazone-mediated PGC1α increased expression and reduces mitochondrial abundance.

In accordance with the previous finding, mitochondrial MitoTracker red staining (Figures 3C, D) of primary adult cardiomyocytes (ACMs) isolated from mice subjected to daily intraperitoneal injections with tesaglitazar (2mg/kg body weight) for 7 days showed lower mitochondrial abundance (-67%; Figure 3D) compared to the ACMs derived from control mice (DMSO-injected). Accordingly, a human cardiomyocyte cell line (AC16) (22) that was treated with tesaglitazar (50μM and 100μM) for 24h showed decreased mitochondrial abundance (-42% for cells treated with 100μM tesaglitazar) (Figures S2A, S2B).

In order to assess whether the reduction in mitochondrial number affected respiratory capacity of cardiomyocytes, we measured oxygen consumption rate (OCR) using the Seahorse Bioscience XF96 Analyzer in primary ACMs derived from mice that were treated with tesaglitazar. This analysis showed impaired mitochondrial respiration as shown by lower basal respiration, maximal respiration, and spare respiratory capacity (Figures 3E, 3F).

PPARα and PPARγ compete for the regulation of the Ppargc1a promoter

In order to confirm that the lack of induction of *Ppargc1a* gene expression upon combined pharmacologic PPARα and PPARγ activation of is not accounted for by off-target effects of rosiglitazone and WY-14643, we infected AC16 cells with recombinant adenoviruses expressing human PPARα (Ad-PPARα) and PPARγ (Ad-PPARγ). In a similar manner with pharmacologic

activation of PPARα and PPARγ, *PPARGC1A* mRNA levels were increased (2.6-fold) in cells treated with Ad-PPARγ (Figure 4A). The positive effect of PPARγ on *PPARGC1A* gene expression was blocked in cells infected with combination of Ad-PPARα and Ad-PPARγ (Figure 4A).

Next, we treated AC16 cells with increasing doses of rosiglitazone (25, 50, and 100μM) and WY-14643 (25, 50, and 100μM) to identify the minimum dose of rosiglitazone that increases *PPARGC1A* expression (Figures S3A-C) and the maximum dose of WY-14643 that does not (Figures S3D-F). This analysis prompted us to select 50μM rosiglitazone and 50μM WY-14643 for further in vitro experiments. Treatment of AC16 cells with 50μM rosiglitazone increased *PPARGC1A* mRNA levels (3.34-fold) (Figure 4B). The same dose, however, did not increase *PPARGC1A* mRNA levels after combination with 50μM WY-14643 (Figure 4B). The inhibitory effect of WY-14643 on rosiglitazone-mediated increase of *PPARGC1A* mRNA levels were partially abolished upon co-administration of 10μM of MK886, a PPARα antagonist (Figure 4B).

As both adenovirus-mediated and combined pharmacological PPARα and PPARγ agonists suppressed PPARγ-mediated upregulation of *PPARGC1A* expression, we tested whether this effect is driven by altered *PPARGC1A* promoter activity. We first tested whether human *PPARGC1A* promoter (obtained from UCSC Genome Browser) contains PPAR response elements (PPREs). Analysis of the *PPARGC1A* promoter sequence up to 2,000bp prior to the transcription initiation site (Genomatix) and sequence comparison between the human and murine *PPARGC1A* promoter sequence (CLUSTAL O 1.2.0 sequence alignment software) (Figure S4A) identified five conserved PPREs that span regions -1631/-1609bp, -1386/-1362bp, -1012/-991bp, -634/-612bp, and -210/-189bp (Figure S4B). To map the region of the human *PPARGC1A* promoter that is responsible for the inhibitory effect of PPARα on PPARγ-mediated upregulation of *PPARGC1A* expression, we generated a panel of *PPARGC1A* promoter deletion mutants (Figure S4C) and cloned this panel into the pGL3-BV luciferase reporter plasmid. We transfected AC16 cells with reporter plasmids containing *PPARGC1A* promoter deletion mutants, pGL3BV-*PPARGC1A*-1631, pGL3BV-*PPARGC1A*-1386, pGL3BV-*PPARGC1A*-1012, and

pGL3BV-*PPARGC1A*-210, and treated them with 50μM rosiglitazone, 50μM WY-14643, or a combination of both. Rosiglitazone increased luciferase activity of the pGL3BV-*PPARGC1A*-1631 (Figure 4C), while it did not have any effect on pGL3BV-*PPARGC1A*-1386 (Figure 4D), pGL3BV-*PPARGC1A*-1012 (Figure 4E) and pGL3BV-*PPARGC1A*-210 (Figure 4F). On the other hand, WY-14643 did not increase luciferase activity in any of the groups (Figures 4C-F). However, the combined treatment with rosiglitazone and WY-14643 prevented rosiglitazone-mediated increase in the activity of the *PPARGC1A*-1631 promoter fragment (Figure 4C). Thus, PPARα and PPARγ compete for regulation of *PPARGC1A* gene expression, and activation of PPARα prevents PPARγ-mediated induction of *PPARGC1A* promoter activity when the PPRE of the -1631/-1609bp region is present.

Our in silico analysis predicted a flanking region of -1631/-1609 in the *PPARGC1A* gene promoter (Figure S4A). In order to assess binding capacity of PPARα and PPRAγ on this region we performed chromatin immunoprecipitation assays using homogenates of hearts from C57BL/6 mice. Significant enrichment of both PPARα and PPRAγ was observed in the *Ppargc1a* gene promoter (Figure 4G). These results suggest that PPARα and PPRAγ can bind to the identical PPRE, and therefore may compete for binding.

Tesaglitazar-decreased cardiac SIRT1 expression and increased PGC1α acetylation

PGC1α activation is controlled via deacetylation of lysine residues by the deacetylase SIRT1 (15). Thus, we determined whether tesaglitazar-mediated cardiac dysfunction is also associated with altered acetylation of PGC1α. Acetylated PGC1α (Ac-PGC1α) that was normalized to heavy IgG and PGC1α input was increased in hearts of mice fed with tesaglitazar-containing chow (2.5-fold; Figures 5A, S5A). In accordance with the increased Ac-PGC1α levels, SIRT1 protein levels were decreased in tesaglitazar-treated mice (-30%; Figures 5B, S5B).

To verify that cardiac SIRT1 decrease is cardiomyocyte-specific, we isolated ACMs from mice that had undergone daily intraperitoneal injections with tesaglitazar (2mg/kg body weight)

for 7 days. SIRT1 protein levels were decreased by 58% in ACMs derived from tesaglitasar-injected mice (Figure 5C, 5D).

Tesaglitazar treatment did not change Ppargc1a and SIRT1 expression in Ppara$^{-/-}$ mice

In order to further test whether combined PPARα and PPARγ activation accounts for the cardiotoxic effects of tesaglitazar, we treated *Ppara*$^{-/-}$ mice with chow diet enriched with tesaglitazar for 6 weeks. The effect of tesaglitazar in cardiac function was less significant in mice with PPARα ablation (Figures 5E, 5D) compared to C57BL/6 mice (Figures 1C, D). In addition, tesaglitazar treatment of *Ppara*$^{-/-}$ mice did not suppress cardiac PGC1a (Figures 5G, H) and SIRT1 protein (Figures 5G, I). The mild decrease in cardiac function of the tesaglitazar-treated *Ppara*$^{-/-}$ mice was associated with increased cardiac expression of *Nppb* (encodes brain natriuretic peptide – BNP; 4.2-fold) and *Col1a1* (encodes collagen, type I, alpha 1; 37-fold) gene expression (Figure 5J). Tesaglitazar-treated *Ppara*$^{-/-}$ mice had increased *Pparg* expression (13-fold), as well as increased *Angptl4*, *Lpl*, *Acox*, and *Cpt1b* expression (Figure 5J). Cardiac expression of *Ucp2*, *Ucp3*, *LpL*, *Acta1* (encodes skeletal a-actin), and *Nppa* (encodes atrial natriuretic peptide – ANP) were not significantly affected (Figure 5J). In addition, *Ppara* ablation was associated with a 5-fold increase on cardiac mtDNA to nuDNA ratio in tesaglitazar-treated mice (Figure 5K).

Resveratrol ameliorated cardiotoxicity of tesaglitazar and maintained its beneficial effects

As tesaglitazar decreased SIRT1 expression and increased Ac-PGC1α levels, we assessed whether pharmacological activation of SIRT1 by resveratrol, and eventually PGC1α would alleviate cardiac toxicity driven by dual PPARα/γ activation. Thus, we treated C57BL/6 mice with chow diet containing tesaglitazar (0.5μmol/kg body weight) or combination of tesaglitazar (0.5μmol/kg body weight) and resveratrol (100mg/kg body weight/day; (23, 24)) for 6 weeks. We did not observe any effect of tesaglitazar alone or in combination with resveratrol in the weight gain rate (Figure S6), plasma glucose (Figure 6A) and triglyceride (Figure 6B) levels. Analysis

with 2D-echocardiography confirmed significant cardiac dysfunction in mice treated with tesaglitazar for 6 weeks (Figures 6C, 6D, Table S2). However, mice treated with combination of tesaglitazar and resveratrol showed significant improvement in cardiac function (FS%) compared to mice treated with tesaglitazar alone (Figures 6C, 6D and Table S2). These findings showed that resveratrol attenuated the tesaglitazar-mediated cardiac dysfunction in C57BL/6 wild type mice. No significant difference was observed in gene expression of markers for cardiac dysfunction or hypertrophy such as *Nppb* and *Acta1* among all treatment groups (Figure S7).

We then tested whether resveratrol-mediated improvement of cardiac function was accompanied by altered cardiac PGC1α activation. Combined treatment of tesaglitazar with resveratrol decreased Ac-PGC1α levels that were elevated in tesaglitazar-fed mice (Figures 6E, S5A). Combined tesaglitazar and resveratrol treatment increased SIRT1 protein levels (58%) compared to tesaglitazar-fed mice (Figures 6F, S5B). Moreover, mice fed on chow diet enriched with tesaglitazar and resveratrol exhibited increased cardiac SIRT3 protein levels (2.3-fold; Figures S8A, S8B) but not SIRT6 protein levels (Figures S8A, S8C).

Combined tesaglitazar and resveratrol treatment improved mitochondrial respiration

Analysis of mitochondrial respiration in isolated primary ACMs from C57BL/6 mice treated with chow diet enriched with tesaglitazar and resveratrol showed restoration of mitochondrial respiration compared to mice treated with tesaglitazar alone, as shown by improved maximal respiration and spare respiratory capacity (Figures 3E, F). As alterations in OCR may correlate with differences in mitochondrial abundance, we performed MitoTracker staining in primary ACMs obtained from mice that received daily intraperitoneal injections with tesaglitazar (2mg/kg body weight/day) or combination of tesaglitazar and resveratrol (100mg/kg body weight/day) for 7 days (Figure 7A). ACMs obtained from mice treated with tesaglitazar alone showed a reduction (-67%) in mitochondrial abundance (Figure 7B). This effect did not occur in ACMs from mice treated with tesaglitazar and resveratrol (Figure 7B). Similarly, AC16 cells that were treated with tesaglitazar for 24h showed lower (-46%) mitochondrial abundance that did not occur following combined

tesaglitazar and resveratrol treatment (Figures S9A, S9B). MtDNA to nuDNA ratio exhibited a trend of reduction in hearts of tesaglitazar-treated mice (-20%), which did not occur in mice that were treated with combined tesaglitazar and resveratrol treatment (Figure 7C).

Mice treated with combination of resveratrol and tesaglitazar had distinct cardiac lipidomic signature

As treatment with tesaglitazar reduced mitochondrial abundance and respiratory capacity, we tested whether it also affects cardiac lipid content. Lipidomic analysis revealed significant differences in most of the lipid classes we assessed. Heat map analysis for the lipid species that we tested followed by hierarchical clustering of those that changed significantly indicated distinct cardiac lipidomic signatures among the three groups of mice (chow-fed control vs. tesaglitazar vs. tesaglitazar + resveratrol) (Figure 7D, Table S3). Specifically, this analysis showed that tesaglitazar increased cardiac triglycerides (6.8-fold), acyl-carnitines (2.3-fold), diacylglycerols (3.1-fold), and phosphatidic acid (30%). Tesaglitazar treatment reduced phosphatidyl-choline (-37%), while there was a strong trend for reduction of monoacyl-glycerols (-40%) and ceramides (-27%). Combined treatment with tesaglitazar and resveratrol restored normal levels of acyl-carnitines, phosphatidic acid, phosphatidyl-choline, monoacyl-glycerols, and ceramides (Table S3).

Combined tesaglitazar and resveratrol treatment lowers plasma lipids and glucose without cardiotoxicity in diabetic and high fat diet-fed mice

We next examined whether the combined treatment with tesaglitazar and resveratrol would exert its beneficial effect in a model of type 2 diabetes. Therefore, *db/db* mice were given chow diet containing no drugs, tesaglitazar, or a combination of tesaglitazar and resveratrol for 6 weeks. No significant effect was observed on weight gain rate between mice treated with tesaglitazar or tesaglitazar and resveratrol (Figure S10A). Combined tesaglitazar and resveratrol treatment corrected hyperlipidemia (Figure 8A) and hyperglycemia (Figure 8B) to a similar extent

with tesaglitazar alone. Despite the similar effect of tesaglitazar alone and combination of tesaglitazar and resveratrol in lowering plasma lipids and glucose, only the single tesaglitazar treatment caused cardiac dysfunction (Figures 8C, D, and Table S4). On the other hand, combined tesaglitazar and resveratrol treatment did not affect cardiac function (Figures 8C, D) and neither did it modulate cardiac mitochondrial abundance (Figure 8E).

As in C57BL/6 mice, *db/db* mice that were fed on chow diet or diet containing combination of tesaglitazar and resveratrol did not have the increase in PGC1α acetylation that was observed in *db/db* mice treated with tesaglitazar alone (Figures 8F, G). Changes in cardiac Ac-PGC1α levels were accompanied by concomitant changes in cardiac SIRT1 protein levels, which were decreased (-39%) with tesaglitazar and restored to normal levels with tesaglitazar and resveratrol (Figure 8H). Moreover, cardiac SIRT6 protein levels were significantly increased in *db/db* mice treated with tesaglitazar and resveratrol as compared to control *db/db* mice but not to those treated with tesaglitazar alone (Figures S10B, C). On the other hand, SIRT3 protein levels were decreased in *db/db* mice treated with tesaglitazar compared to chow-fed *db/db* mice, but resveratrol supplementation did not correct SIRT3 levels in cardiac tissue of *db/db* mice (Figures S10B, D).

We also treated C57BL/6 mice with high fat diet (HFD) alone or HFD containing tesaglitazar (0.5μmol/kg body weight) for 6 weeks. Both mouse groups had similar weight gain rates (Figures S10E, F). Plasma glucose and TGs were significantly lower in mice that were fed with HFD and tesaglitazar compared to control HFD-fed mice (Figures 9A, B). Tesaglitazar treatment compromised systolic cardiac function (Figures 9C, D and Table S5). Tesaglitazar treatment also decreased cardiac *PPARGC1a* mRNA (-63%) (Figure 9E) and protein levels (-31%) (Figure 9F, G), as well as increased Ac-PGC1α (4.3-fold; Figures 9F, H). In accordance with the increased Ac-PGC1α levels, cardiac SIRT1 protein levels were decreased in HFD-tesaglitazar treated mice (-61%; Figures 9F, I).

Resveratrol abolished its cardioprotective effect in tesaglitazar-treated aMHC-Sirt1$^{-/-}$ mice

We sought to confirm involvement of SIRT1 in mediating the cardioprotective effect of resveratrol in mice treated with tesaglitazar. Therefore, we treated C57BL/6 and *aMHC-Sirt1*$^{-/-}$ with chow diet containing combination of tesaglitazar and resveratrol. Unlike the negation of the toxic effects of tesaglitazar by resveratrol in C57BL/6 mice, the same treatment did not rescue cardiac function in *aMHC-Sirt1*$^{-/-}$ mice (Figures 9J, K). Thus, cardiomyocyte SIRT1 is crucial in mediating the protective effect of resveratrol.

DISCUSSION

Agonists for PPARs are used to treat hyperglycemia and hypertriglyceridemia in patients with type 2 diabetes. Despite these benefits, some PPARγ agonists, such as rosiglitazone and pioglitazone, have been associated with increased heart failure due to direct or indirect cardiac effects, such as fluid retention (3). In the last 15 years, potential cardiovascular effects of rosiglitazone have become controversial despite its insulin-sensitizing benefits. Various studies had concluded that thiazolidinediones (TZDs) increase risk for heart failure due to direct cardiovascular effects or other indirect effects. However, some of these studies acknowledged only a small increase in heart failure incidents in patients on rosiglitazone and simply advised patients and health care providers to be aware of the risks. A meta-analysis of randomized trials associated rosiglitazone with increased risk for myocardial infarctions (25). The PROactive study and a meta-analysis of randomized trials showed that although pioglitazone treatment of patients with diabetes increases heart failure incidence, subsequent all-cause mortality is decreased (26, 27). Compared to pioglitazone, rosiglitazone appeared to be associated with a higher risk of heart failure and other cardiovascular events (28). However, the RECORD trial showed that rosiglitazone treatment is associated with an increased risk for heart failure, but not for myocardial infarctions, stroke, or cardiovascular mortality (29, 30). A 2010 AHA/ACCF Science Advisory reevaluated the cardiovascular risks of TZDs and concluded that a link between rosiglitazone and heart failure could not be established (31). Thus, in 2013 the FDA removed restrictions on rosiglitazone.

Efforts to discover new PPAR agonists without adverse effects led to the development of dual agonists (glitazars) that activate both PPARα and PPARγ, thus combining successfully (4) the lipid-lowering effects of PPARα with the insulin sensitizing effects of PPARγ. Dual PPARα/γ agonists have various actions, which in several cases deviate between mice and humans. Aleglitazar was protective in mouse cardiomyocytes exposed to high glucose levels in vitro (32) in a PPARα- and PPARγ-dependent manner. Another PPARα/γ agonist, CG301269, also showed beneficial metabolic effects in rodents (33). In the same study, administration of CG301269 in a mouse model of myocardial ischemia/reperfusion did not aggravate further heart failure. In contrast, another dual PPARα/γ agonist, LY510929, which exerted anti-hyperlipidemic and anti-hyperglycemic effects in mice and rats (34), caused left ventricular hypertrophy in rats when was given for 2 weeks (35).

Human studies showed that dual agonists have limited therapeutic benefits. Patients with type 2 diabetes and recent acute coronary syndrome did not show improvement in cardiovascular outcomes when treated with aleglitazar (36). Another dual agonist, saroglitazar, has been approved for clinical use but there is a precautionary statement for patients with diabetes and congestive heart failure (37). Other glitazars, such as tesaglitazar (5) and muraglitazar (6) were abandoned when clinical trials showed either increased risk for cardiovascular events or other adverse effects. However, the mechanisms that mediate these adverse outcomes remain unclear. Our study shows that the toxic effect of tesaglitazar, a dual PPARα/γ agonist, in both healthy C57BL/6 and diabetic *db/db* mice is accounted for by inhibition of both expression and acetylation/deactivation of cardiac PGC1α. PGC1α is the transcriptional co-activator of PPARs and controls FAO-related gene expression (38) and mitochondrial biogenesis (14).

PPARs respond to various endogenous ligands such as steroids, retinoids, cholesterol metabolites, and dietary lipids (10). Upon binding of the ligand, PPARs heterodimerize with retinoid X receptors (RXR) and bind to cis-acting DNA-elements (PPREs) to increase gene transcription. PPARs have broad tissue distribution and promote lipid metabolism in several organs including the heart (39). FAO is the primary source of cardiac ATP and its inhibition is

associated with cardiac dysfunction (13, 40). While PPARα promotes FA uptake and FAO (8), PPARγ increases cardiac lipid accumulation (41). PPARγ can also induce cardiac FAO-related gene expression (41) when PPARα is inhibited (11, 13). However, how PPARα prevents PAPRγ-mediated induction of cardiac FAO and why combined activation of both PPARα and PPARγ causes cardiac dysfunction remained elusive. One given explanation is that combined increase in PPARγ-driven insulin sensitization and glucose uptake in the setting of higher PPARα-induced FA metabolism causes combined gluco-lipo-toxicity (42). In the present study, we portray a different explanation; that toxicity by combined PPARα/γ activation leads to inhibition of SIRT1 and PGC1α and reduces mitochondrial abundance.

Our previous studies have indicated that combined PPARα and PPARγ activation might compromise cardiac function. In those studies, we investigated the cardiac effects of PPARγ activation (11, 13, 41) and showed that cardiomyocyte-specific overexpression of PPARγ causes intramyocardial lipid accumulation and cardiac dysfunction (41). We had shown that the observed excessive lipid accumulation may account for some components of cardiac dysfunction, such as beta-adrenergic desensitization (13) and arrhythmia (43). Other studies had shown that pharmacologic activation or constitutive cardiomyocyte expression of PPARα cause cardiac dysfunction (8, 44). However, constitutive PPARγ expression in cardiomyocytes of *Ppara*$^{-/-}$ mice did not cause cardiac dysfunction despite increased myocardial lipid content (11), indicating a toxic role for cardiac PPARα when PPARγ is activated as well. Moreover, rosiglitazone-mediated PPARγ activation promotes cardiomyocyte hypertrophy in vitro (45), while fenofibrate-mediated PPARα activation has the opposite effect in isolated cardiomyocytes and rescues mitochondrial function (46). Activation of PPARs relies on availability of FAs that are released either via LpL-mediated hydrolysis of lipoprotein triglycerides (47) or from intracellular triglycerides via ATGL-mediated lipolysis (48). Thus, cardiac dysfunction in mice that overexpress cardiomyocyte PPARγ may be partially due to FA-mediated PPARα activation, which does not occur in aMHC-*Pparg;Ppara*$^{-/-}$ mice (11). Tesaglitazar-induced cardiac dysfunction was associated with accumulation of cardiac lipids including lipids that have been linked with cardiac lipotoxicity, such

as acyl-carnitines and diacylglycerols (11, 49). Thus, combined activation of PPARα and PPARγ may cause cardiac toxicity due to elevated toxic lipid species. Future studies comparing the cardiovascular effects of treatment with rosiglitazone alone and combined treatment with rosiglitazone and PPARα antagonists are warranted to elucidate further the mechanism that underlies toxicity by dual activation of PPARα and PPARγ. Nevertheless, the controversy from clinical studies with TZDs may source from differential levels of PPARα activation.

Besides lipotoxicity, our study identified reduced mitochondrial function as another component of cardiac toxicity with tesaglitazar. Activation of PPARα in mice that were also treated with the PPARγ agonist, rosiglitazone, prevented rosiglitazone-mediated increase of *Ppargc1a* and FAO-related gene expression and decreased mitochondrial number. Accordingly, we show that pharmacologic or genetic activation of PPARγ induces *Ppargc1a* expression, which does not occur when both PPARα and PPARγ are activated. Moreover, we revealed that both PPARα and PPARγ can bind on the -1631/-1609 flanking region of the *Ppargc1a* gene promoter and compete for regulating promoter's activity. All the above, are consistent with our previous findings showing that pharmacologic activation of PPARα in aMHC-*Pparg*$^{-/-}$ mice reduced cardiac expression of *Ppargc1a* and FA metabolism-related genes (11). Similarly, PPARγ activation in *Ldlr*$^{-/-}$ mice fed with HFD, which increases cardiac PPARα levels (50, 51), reduces *Ppargc1a* expression and causes cardiac hypertrophy (52). Conversely, we have shown that activation of cardiac PPARγ in mice with low levels of cardiac PPARα expression increases *Ppargc1a* expression profoundly (13). Similarly, treatment of *Ppara*$^{-/-}$ mice with tesaglitazar had a milder effect in cardiac function and did not inhibit PGC1α and SIRT1. Moreover, cardiac dysfunction due to tesaglitazar treatment did not increase expression of genes for cardiac hypertrophy. This suggests that cardiac dysfunction at the early stage of tesaglitazar treatment is an acute effect of the drug that can still be reversed. Tesaglitazar increased *Ppard*, which has also been involved in the regulation of cardiac FAO (53). Upregulation of cardiac PPARδ expression correlates with increased expression of UCP3, which is a PPARδ target gene in cardiac (53) and skeletal muscle (54, 55). Additional studies are needed in order to evaluate potential compensatory activation of PPARδ

upon inhibition of PGC1α, as well as to elucidate whether long-term tesaglitazar treatment causes irreversible cardiac dysfunction and remodeling, accompanied by increased expression of heart failure markers.

Activation of PGC1α within a critical threshold is crucial for healthy cardiac function. Nevertheless, both reduced and highly increased PGC1α levels have been associated with cardiac toxicity. More specifically, cardiac PGC1α expression is decreased in rodents and humans with heart failure (56). Accordingly, *Ppargc1a*$^{-/-}$ mice develop moderate cardiac dysfunction (38), which is aggravated with pressure overload (57). The milder cardiac phenotype at baseline may be accounted for by compensatory function of PGC1β, which shares functional redundancy with PGC1α. Indeed, combined knock-out of both *Ppargc1a* and *Ppargc1b* inhibits perinatal cardiac mitochondrial biogenesis and causes cardiomyopathy and post-partum death (58). On the other hand, overexpression of cardiomyocyte PGC1α also causes cardiac dysfunction (14). The cardiotoxic effect of the long-term increase of PGC1α is associated with impaired mitochondrial biogenesis and function (14). Nevertheless, the same study reported that cardiac function is normal in transgenic lines with lower PGC1α constitutive expression. Accordingly, short-term PGC1α overexpression in cultured cardiomyocytes improved mitochondrial biogenesis and oxidative respiration, which has been associated with better cardiac function. Thus, the level of cardiomyocyte PGC1α activation seems to be critical for determining its protective or aggravating role.

The role of PGC1α inhibition as a key event that mediates the cardiotoxic effect of dual PPARα/γ activation is a novel finding. Our data show that dual-PPARα/γ activation reduces both expression and activation of cardiac PGC1α by enhancing acetylation. In addition, it lowers mitochondrial abundance, which is accompanied by lower OCR in cardiomyocytes. It has been suggested that lower acetylation of cardiac PGC1α may account for the shift from glycolysis to FAO that occurs during maturation (59). PGC1α acetylation is controlled by the deacetylase SIRT1 (15), which was reduced in the hearts of mice treated with the dual PPARα/γ agonist. SIRT1 inhibition has been associated with cardiac dysfunction in various forms of cardiac stress,

such as ischemia/reperfusion (I/R) and cardiac aging (60), whereas young cardiac-specific *Sirt1*$^{-/-}$ mice exhibit normal cardiac function (61). SIRT1 and PGC1α are activated by resveratrol, which is a polyphenolic compound with anti-oxidant and anti-inflammatory properties (62). The beneficial cardiac effects of resveratrol have been attributed, at least in part, to the activation of SIRT1 (63). Both resveratrol and SIRT1, have been associated with mitochondrial biogenesis (64). Inhibition of SIRT1 has been correlated with diabetes-related cardiometabolic abnormalities, while a protective role has been suggested for activated SIRT1 (65). Resveratrol prevents mitochondrial dysfunction in rats with type 2 diabetes (66, 67). Also, resveratrol attenuates cardiac injury in rats with type 1 diabetes through SIRT1-mediated regulation of mitochondrial function and PGC1α deacetylation (68). The mitochondrial SIRT3 is also increased in mice treated with tesaglitazar and resveratrol, although it was not decreased in tesaglitazar-treated mice. The expression of SIRT6 was not altered in any of the groups we tested, except the *db/db* mice that had increased levels upon combined treatment with tesaglitazar and resveratrol. However, as SIRT6 increases PGC1α acetylation indirectly (69), this change in *db/db* mice cannot explain lower acetylation levels. Thus, SIRT1 seems to be the main isoform with altered expression that may explain increased acetylation of PGC1α in tesaglitazar-treated mice, which is reversed with combined tesaglitazar and resveratrol treatment. Future studies that will use more SIRT1 activators, such as metformin (70, 71) and SRT1720 (72), are warranted in order to elucidate further to elucidate further the interplay among fatty acid oxidation, altered NAD^+:NADH ratio, SIRT1, SIRT3, and acetyl-transferases, such as GCN5 (73), in regulating acetylation and activation of PGC1α along with acetylation of mitochondrial proteins.

In summary, our previous (11, 13) and present findings suggest that dual PPARα/γ-mediated inactivation of the “metabolic network”, which involves SIRT1 and PGC1α, may account for cardiac toxicity by compromising cardiac mitochondrial biology and energy homeostasis (Figure 9L). Our observations can explain the mechanism that underlies the cardiotoxic effects of one of the dual PPARα/γ agonists, tesaglitazar. We show for the first time that the negative effects of tesaglitazar can be effectively reversed upon combined administration with resveratrol.

Combined treatment with resveratrol and tesaglitazar maintained the beneficial anti-hyperlipidemic and anti-hyperglycemic effects of tesaglitazar that were independent from resveratrol, which cannot reduce plasma triglyceride levels (74). Thus, combination of dual PPARα/γ agonists and activation of the SIRT1-PGC1α axis holds promise for future therapeutic applications in type 2 diabetes if the same observations are reproduced with other dual PPARα/γ dual agonists. Moreover, our study provides a guide for design of future PPAR agonists that should be screened for lack of inhibition of PGC1α activity.

METHODS

Chemical reagents - All chemical reagents were obtained from SIGMA unless otherwise noted. Rosiglitazone and WY-14643 were purchased from Enzo Life Sciences.

Animals – Male C57BL/6 (6 weeks), *db/db* (6 weeks) and *Ppara*$^{-/-}$ (8 weeks) mice were obtained from the Jackson Laboratory and fed with chow diet supplemented with tesaglitazar or combination of tesaglitazar and resveratrol. The aMHC-*Sirt1*$^{-/-}$ (6 weeks; male) mice have been previously described (75). More information is provided in the Supplementary Materials.

Cells - The human ventricular cardiomyocyte cell line (AC16) (22) was maintained in complete DMEM/F-12 medium at 37°C and 5%CO_2.

Echocardiography analysis - Cardiac function of anesthetized mice was assessed by two-dimensional (2D) echocardiography (VisualSonics-Vevo2100) as previously described (12, 76).

Adenoviruses - Recombinant adenoviruses expressing human PPARγ (Ad-PPARγ) and control GFP (Ad-GFP) were generated as described previously (77). Adenovirus expressing human PPARα (Ad-PPARα) was purchased from Vector Biolabs (Philadelphia, PA, USA). Infections of AC16 cells were performed as described previously (77).

Transfection and luciferase assay - FuGENE 6 Transfection Reagent (Promega) was used to transfect AC16 cells, which were seeded in 96-well-plates (50,000 cells), with human *PPARGC1A* promoter containing pGL3-BV plasmids according to manufacturer's protocols. More detailed information is included in the Supplementary Materials. Luciferase activity was quantified with Infinite® M1000 PRO plate reader.

Chromatin immunoprecipitation - Heart tissue was cross-linked with formaldehyde. The nuclear fraction was isolated and sonicated to generate a chromatin solution that was then used for immunoprecipitation with anti-PPARα antibody (Cayman 101710), anti-PPARγ (Cell Signaling

#2443) and control IgG (Cell Signaling 2729). The corrected genomic fragments were validated with quantitative PCR with primers described in Table S7.

MitoTracker Red staining - Cells were plated on sterile glass chamber slides and were exposed to MitoTracker Red (Molecular Probes) as we have described previously (78). Description of the procedure and analysis is included in the Supplementary Materials.

Mitochondrial abundance - Mitochondrial abundance was determined by the ratio of mitochondrial copy number (mtDNA) to nucleic DNA (nuDNA). Both mtDNA and nuDNA were measured by quantitative real-time PCR. For mtDNA we used primers for detecting *CoxII* gene expression and for nuDNA we used primers for *b-globin* (Table S7).

RNA purification and gene expression analysis - Total RNA was purified from cells or hearts using the TRIzol reagent (Invitrogen). cDNA synthesis and analysis with SYBR Green Reagent and quantitative real-time PCR were performed as described previously (12). More detailed information is included in the Supplementary Materials.

Protein purification and analysis - Freshly isolated hearts and cells were homogenized in RIPA buffer containing protease/phosphatase inhibitors (Pierce-Biotechnology). Total protein extracts (30-40μg) were analyzed with SDS-PAGE and Western Blotting. Detailed information is included in the Supplementary Materials. Complete list of antibodies used can be found in Table S6 in the Supplementary Materials.

Immunoprecipitation (IP) - Purified protein lysates (100μg) were precleared with protein A/G-agarose beads. The lysates were incubated with antibodies (2μg/100μg lysate) overnight at 4°C under gentle rotation. Detailed information is included in the Supplementary Materials

Oxygen consumption rate analysis - Oxygen consumption rate (OCR) was determined using a Seahorse Bioscience XF96 Extracellular Flux Analyzer. Primary ACMs isolated from 6-week old mice were plated (3000 cells/well) in XF96 Seahorse® plates. Intact cellular respiration was assayed prior to and after administration of the mitochondrial inhibitors oligomycin, carbonyl cyanide-p-trifluoromethoxyphenylhydrazone (FCCP), and antimycin A / rotenone. Calculations were made with the Wave 2.3 Software. Detailed information is included in the Supplementary Materials.

Lipidomic analysis - Lipids were extracted via chloroform-methanol extraction, spiked with appropriate internal standards, and analyzed using a 6490 Triple Quadrupole LC/MS system (Columbia University). Detailed description is included in the Supplementary Materials.

Statistics - All group comparisons have been performed by 1-way ANOVA analysis or by non-paired two-tailed Student's t-test. Multiple comparisons in 1-way ANOVA were assessed using Tukey post-hoc test. Values represent means $\pm$ SEM. Sample size and p values are provided in the figure legends. A P value less than 0.05 was considered significant.

Study Approval - All procedures involving animals were approved by the Institutional Animal Care and Use Committees at Temple University (Philadelphia, PA) and Columbia University (New York, NY).

AUTHOR CONTRIBUTIONS

The research plan was conceived by KD and CK. The methods were performed by CK, IDK, SO, MJL, YY, EAG, YT, WM, AC, DS and PCS. The analysis of the results was performed by CK, IDK, SO, MJL, YY, EAG and KD. Experiments were performed by CK, IDK, SO, MJL, YY, EAG, CJP, YT, WM, AC, DS and MC. Funding was obtained by KD, IJG and IDK. The original draft was written by CK, IDK and KD while CK, IDK, KD, IJG, SO, MJL, YY, EAG, CJP, YT, PCS, MC, JS and MM reviewed and edited it. Finally, research supervision was conducted by KD and IJG. CK and IDK share first author position for equal contribution in performing experimental procedures as well in writing and editing of the manuscript.

ACKNOWLEDGEMENTS

Charikleia Kalliora was a MSc student of the “Molecular Basis of Human Diseases” graduate program of the Medical School, University of Crete, Greece. We would like to thank Mesele-Christina Valenti and Brett Brown for technical assistance.

FUNDING

This work was supported by a National Heart Lung Blood Institute-NIH “Pathway to Independence” R00 award (HL112853), HL130218, and a grant from the W. W. Smith Charitable Trust (KD), HL073029, and HL135987 (IJG). IDK was supported by the American Heart Association and the Kahn Family Post-Doctoral Fellowship in Cardiovascular Research (18POST34060150).

COMPETING INTERESTS

The authors have declared that no conflict of interest exists.

REFERENCES

1. Fruchart JC. Peroxisome proliferator-activated receptor-alpha (PPARalpha): at the crossroads of obesity, diabetes and cardiovascular disease. *Atherosclerosis.* 2009;205(1):1-8.
2. Heikkinen S, Auwerx J, and Argmann CA. PPARgamma in human and mouse physiology. *Biochim Biophys Acta.* 2007;1771(8):999-1013.
3. Seferovic PM, Petrie MC, Filippatos GS, Anker SD, Rosano G, Bauersachs J, Paulus WJ, Komajda M, Cosentino F, de Boer RA, et al. Type 2 diabetes mellitus and heart failure: a position statement from the Heart Failure Association of the European Society of Cardiology. *European journal of heart failure.* 2018;20(5):853-72.
4. Chatterjee S, Majumder A, and Ray S. Observational study of effects of Saroglitazar on glycaemic and lipid parameters on Indian patients with type 2 diabetes. *Scientific reports.* 2015;5(7706.
5. Goldstein BJ, Rosenstock J, Anzalone D, Tou C, and Ohman KP. Effect of tesaglitazar, a dual PPAR alpha/gamma agonist, on glucose and lipid abnormalities in patients with type 2 diabetes: a 12-week dose-ranging trial. *Current medical research and opinion.* 2006;22(12):2575-90.
6. Nissen SE, Wolski K, and Topol EJ. Effect of muraglitazar on death and major adverse cardiovascular events in patients with type 2 diabetes mellitus. *Jama.* 2005;294(20):2581-6.
7. Madrazo JA, and Kelly DP. The PPAR trio: regulators of myocardial energy metabolism in health and disease. *J Mol Cell Cardiol.* 2008;44(6):968-75.
8. Finck BN, Lehman JJ, Leone TC, Welch MJ, Bennett MJ, Kovacs A, Han X, Gross RW, Kozak R, Lopaschuk GD, et al. The cardiac phenotype induced by PPARalpha overexpression mimics that caused by diabetes mellitus. *The Journal of clinical investigation.* 2002;109(1):121-30.

9. Park SY, Cho YR, Finck BN, Kim HJ, Higashimori T, Hong EG, Lee MK, Danton C, Deshmukh S, Cline GW, et al. Cardiac-specific overexpression of peroxisome proliferator-activated receptor-alpha causes insulin resistance in heart and liver. *Diabetes.* 2005;54(9):2514-24.

10. Pol CJ, Lieu M, and Drosatos K. PPARs: Protectors or Opponents of Myocardial Function? *PPAR research.* 2015;2015(835985.

11. Son NH, Yu S, Tuinei J, Arai K, Hamai H, Homma S, Shulman GI, Abel ED, and Goldberg IJ. PPARgamma-induced cardiolipotoxicity in mice is ameliorated by PPARalpha deficiency despite increases in fatty acid oxidation. *J Clin Invest.* 2010;120(10):3443-54.

12. Drosatos K, Pollak NM, Pol CJ, Ntziachristos P, Willecke F, Valenti MC, Trent CM, Hu Y, Guo S, Aifantis I, et al. Cardiac Myocyte KLF5 Regulates Ppara Expression and Cardiac Function. *Circulation research.* 2016;118(2):241-53.

13. Drosatos K, Khan RS, Trent CM, Jiang H, Son NH, Blaner WS, Homma S, Schulze PC, and Goldberg IJ. Peroxisome proliferator-activated receptor-gamma activation prevents sepsis-related cardiac dysfunction and mortality in mice. *Circ Heart Fail.* 2013;6(3):550-62.

14. Lehman JJ, Barger PM, Kovacs A, Saffitz JE, Medeiros DM, and Kelly DP. Peroxisome proliferator-activated receptor gamma coactivator-1 promotes cardiac mitochondrial biogenesis. *J Clin Invest.* 2000;106(7):847-56.

15. Rodgers JT, Lerin C, Haas W, Gygi SP, Spiegelman BM, and Puigserver P. Nutrient control of glucose homeostasis through a complex of PGC-1alpha and SIRT1. *Nature.* 2005;434(7029):113-8.

16. Michan S, and Sinclair D. Sirtuins in mammals: insights into their biological function. *The Biochemical journal.* 2007;404(1):1-13.

17. Fagerberg B, Edwards S, Halmos T, Lopatynski J, Schuster H, Stender S, Stoa-Birketvedt G, Tonstad S, Halldorsdottir S, and Gause-Nilsson I. Tesaglitazar, a novel dual peroxisome proliferator-activated receptor alpha/gamma agonist, dose-dependently

improves the metabolic abnormalities associated with insulin resistance in a non-diabetic population. *Diabetologia.* 2005;48(9):1716-25.

18. Bays H, McElhattan J, Bryzinski BS, and Group GS. A double-blind, randomised trial of tesaglitazar versus pioglitazone in patients with type 2 diabetes mellitus. *Diabetes & vascular disease research.* 2007;4(3):181-93.
19. Wallenius K, Kjellstedt A, Thalen P, Lofgren L, and Oakes ND. The PPAR alpha / gamma Agonist, Tesaglitazar, Improves Insulin Mediated Switching of Tissue Glucose and Free Fatty Acid Utilization In Vivo in the Obese Zucker Rat. *PPAR research.* 2013;2013(305347.
20. Finck BN, and Kelly DP. PGC-1 coactivators: inducible regulators of energy metabolism in health and disease. *J Clin Invest.* 2006;116(3):615-22.
21. Wu Z, Puigserver P, Andersson U, Zhang C, Adelmant G, Mootha V, Troy A, Cinti S, Lowell B, Scarpulla RC, et al. Mechanisms controlling mitochondrial biogenesis and respiration through the thermogenic coactivator PGC-1. *Cell.* 1999;98(1):115-24.
22. Davidson MM, Nesti C, Palenzuela L, Walker WF, Hernandez E, Protas L, Hirano M, and Isaac ND. Novel cell lines derived from adult human ventricular cardiomyocytes. *Journal of molecular and cellular cardiology.* 2005;39(1):133-47.
23. Ji G, Wang Y, Deng Y, Li X, and Jiang Z. Resveratrol ameliorates hepatic steatosis and inflammation in methionine/choline-deficient diet-induced steatohepatitis through regulating autophagy. *Lipids in health and disease.* 2015;14(134.
24. Sulaiman M, Matta MJ, Sunderesan NR, Gupta MP, Periasamy M, and Gupta M. Resveratrol, an activator of SIRT1, upregulates sarcoplasmic calcium ATPase and improves cardiac function in diabetic cardiomyopathy. *American journal of physiology Heart and circulatory physiology.* 2010;298(3):H833-43.
25. Nissen SE, and Wolski K. Effect of rosiglitazone on the risk of myocardial infarction and death from cardiovascular causes. *The New England journal of medicine.* 2007;356(24):2457-71.

26. Erdmann E, Charbonnel B, Wilcox RG, Skene AM, Massi-Benedetti M, Yates J, Tan M, Spanheimer R, Standl E, Dormandy JA, et al. Pioglitazone use and heart failure in patients with type 2 diabetes and preexisting cardiovascular disease: data from the PROactive study (PROactive 08). *Diabetes care.* 2007;30(11):2773-8.

27. Lincoff AM, Wolski K, Nicholls SJ, and Nissen SE. Pioglitazone and risk of cardiovascular events in patients with type 2 diabetes mellitus: a meta-analysis of randomized trials. *Jama.* 2007;298(10):1180-8.

28. Graham DJ, Ouellet-Hellstrom R, MaCurdy TE, Ali F, Sholley C, Worrall C, and Kelman JA. Risk of acute myocardial infarction, stroke, heart failure, and death in elderly Medicare patients treated with rosiglitazone or pioglitazone. *Jama.* 2010;304(4):411-8.

29. Home PD, Pocock SJ, Beck-Nielsen H, Curtis PS, Gomis R, Hanefeld M, Jones NP, Komajda M, McMurray JJ, and Team RS. Rosiglitazone evaluated for cardiovascular outcomes in oral agent combination therapy for type 2 diabetes (RECORD): a multicentre, randomised, open-label trial. *Lancet.* 2009;373(9681):2125-35.

30. Mahaffey KW, Hafley G, Dickerson S, Burns S, Tourt-Uhlig S, White J, Newby LK, Komajda M, McMurray J, Bigelow R, et al. Results of a reevaluation of cardiovascular outcomes in the RECORD trial. *American heart journal.* 2013;166(2):240-9 e1.

31. Kaul S, Bolger AF, Herrington D, Giugliano RP, and Eckel RH. Thiazolidinedione drugs and cardiovascular risks: a science advisory from the American Heart Association and American College of Cardiology Foundation. *Circulation.* 2010;121(16):1868-77.

32. Chen Y, Chen H, Birnbaum Y, Nanhwan MK, Bajaj M, Ye Y, and Qian J. Aleglitazar, a dual peroxisome proliferator-activated receptor-alpha and -gamma agonist, protects cardiomyocytes against the adverse effects of hyperglycaemia. *Diabetes & vascular disease research.* 2017;14(2):152-62.

33. Jeong HW, Lee JW, Kim WS, Choe SS, Kim KH, Park HS, Shin HJ, Lee GY, Shin D, Lee H, et al. A newly identified CG301269 improves lipid and glucose metabolism without body

weight gain through activation of peroxisome proliferator-activated receptor alpha and gamma. *Diabetes.* 2011;60(2):496-506.

34. Willson TM, Cobb JE, Cowan DJ, Wiethe RW, Correa ID, Prakash SR, Beck KD, Moore LB, Kliewer SA, and Lehmann JM. The structure-activity relationship between peroxisome proliferator-activated receptor gamma agonism and the antihyperglycemic activity of thiazolidinediones. *Journal of medicinal chemistry.* 1996;39(3):665-8.

35. Engle SK, Solter PF, Credille KM, Bull CM, Adams S, Berna MJ, Schultze AE, Rothstein EC, Cockman MD, Pritt ML, et al. Detection of left ventricular hypertrophy in rats administered a peroxisome proliferator-activated receptor alpha/gamma dual agonist using natriuretic peptides and imaging. *Toxicological sciences : an official journal of the Society of Toxicology.* 2010;114(2):183-92.

36. Lincoff AM, Tardif JC, Schwartz GG, Nicholls SJ, Ryden L, Neal B, Malmberg K, Wedel H, Buse JB, Henry RR, et al. Effect of aleglitazar on cardiovascular outcomes after acute coronary syndrome in patients with type 2 diabetes mellitus: the AleCardio randomized clinical trial. *Jama.* 2014;311(15):1515-25.

37. Discovery Z. Lipaglyn Product Information. 2013.

38. Arany Z, He H, Lin J, Hoyer K, Handschin C, Toka O, Ahmad F, Matsui T, Chin S, Wu PH, et al. Transcriptional coactivator PGC-1 alpha controls the energy state and contractile function of cardiac muscle. *Cell Metab.* 2005;1(4):259-71.

39. Auboeuf D, Rieusset J, Fajas L, Vallier P, Frering V, Riou JP, Staels B, Auwerx J, Laville M, and Vidal H. Tissue distribution and quantification of the expression of mRNAs of peroxisome proliferator-activated receptors and liver X receptor-alpha in humans: no alteration in adipose tissue of obese and NIDDM patients. *Diabetes.* 1997;46(8):1319-27.

40. Neubauer S. The failing heart--an engine out of fuel. *The New England journal of medicine.* 2007;356(11):1140-51.

41. Son NH, Park TS, Yamashita H, Yokoyama M, Huggins LA, Okajima K, Homma S, Szabolcs MJ, Huang LS, and Goldberg IJ. Cardiomyocyte expression of PPARgamma leads to cardiac dysfunction in mice. *J Clin Invest.* 2007;117(10):2791-801.

42. Nolan CJ, Ruderman NB, Kahn SE, Pedersen O, and Prentki M. Insulin resistance as a physiological defense against metabolic stress: implications for the management of subsets of type 2 diabetes. *Diabetes.* 2015;64(3):673-86.

43. Morrow JP, Katchman A, Son NH, Trent CM, Khan R, Shiomi T, Huang H, Amin V, Lader JM, Vasquez C, et al. Mice With Cardiac Overexpression of Peroxisome Proliferator-Activated Receptor gamma Have Impaired Repolarization and Spontaneous Fatal Ventricular Arrhythmias. *Circulation.* 2011;124(25):2812-21.

44. Zungu M, Young ME, Stanley WC, and Essop MF. Chronic treatment with the peroxisome proliferator-activated receptor alpha agonist Wy-14,643 attenuates myocardial respiratory capacity and contractile function. *Molecular and cellular biochemistry.* 2009;330(1-2):55-62.

45. Pharaon LF, El-Orabi NF, Kunhi M, Al Yacoub N, Awad SM, and Poizat C. Rosiglitazone promotes cardiac hypertrophy and alters chromatin remodeling in isolated cardiomyocytes. *Toxicology letters.* 2017;280(151-8.

46. Kar D, and Bandyopadhyay A. Targeting Peroxisome Proliferator Activated Receptor alpha (PPAR alpha) for the Prevention of Mitochondrial Impairment and Hypertrophy in Cardiomyocytes. *Cellular physiology and biochemistry : international journal of experimental cellular physiology, biochemistry, and pharmacology.* 2018;49(1):245-59.

47. Ziouzenkova O, Perrey S, Asatryan L, Hwang J, MacNaul KL, Moller DE, Rader DJ, Sevanian A, Zechner R, Hoefler G, et al. Lipolysis of triglyceride-rich lipoproteins generates PPAR ligands: evidence for an antiinflammatory role for lipoprotein lipase. *Proc Natl Acad Sci U S A.* 2003;100(5):2730-5.

48. Lahey R, Wang X, Carley AN, and Lewandowski ED. Dietary fat supply to failing hearts determines dynamic lipid signaling for nuclear receptor activation and oxidation of stored triglyceride. *Circulation.* 2014;130(20):1790-9.

49. Drosatos K, Bharadwaj KG, Lymperopoulos A, Ikeda S, Khan R, Hu Y, Agarwal R, Yu S, Jiang H, Steinberg SF, et al. Cardiomyocyte lipids impair beta-adrenergic receptor function via PKC activation. *Am J Physiol Endocrinol Metab.* 2011;300(3):E489-99.

50. Li Y, Cheng L, Qin Q, Liu J, Lo WK, Brako LA, and Yang Q. High-fat feeding in cardiomyocyte-restricted PPARdelta knockout mice leads to cardiac overexpression of lipid metabolic genes but fails to rescue cardiac phenotypes. *J Mol Cell Cardiol.* 2009;47(4):536-43.

51. Cole MA, Abd Jamil AH, Heather LC, Murray AJ, Sutton ER, Slingo M, Sebag-Montefiore L, Tan SC, Aksentijevic D, Gildea OS, et al. On the pivotal role of PPARalpha in adaptation of the heart to hypoxia and why fat in the diet increases hypoxic injury. *FASEB J.* 2016;30(8):2684-97.

52. Verschuren L, Wielinga PY, Kelder T, Radonjic M, Salic K, Kleemann R, van Ommen B, and Kooistra T. A systems biology approach to understand the pathophysiological mechanisms of cardiac pathological hypertrophy associated with rosiglitazone. *BMC medical genomics.* 2014;7(35.

53. Cheng L, Ding G, Qin Q, Huang Y, Lewis W, He N, Evans RM, Schneider MD, Brako FA, Xiao Y, et al. Cardiomyocyte-restricted peroxisome proliferator-activated receptor-delta deletion perturbs myocardial fatty acid oxidation and leads to cardiomyopathy. *Nat Med.* 2004;10(11):1245-50.

54. Chevillotte E, Rieusset J, Roques M, Desage M, and Vidal H. The regulation of uncoupling protein-2 gene expression by omega-6 polyunsaturated fatty acids in human skeletal muscle cells involves multiple pathways, including the nuclear receptor peroxisome proliferator-activated receptor beta. *The Journal of biological chemistry.* 2001;276(14):10853-60.

55. Dressel U, Allen TL, Pippal JB, Rohde PR, Lau P, and Muscat GE. The peroxisome proliferator-activated receptor beta/delta agonist, GW501516, regulates the expression of genes involved in lipid catabolism and energy uncoupling in skeletal muscle cells. *Molecular endocrinology.* 2003;17(12):2477-93.

56. Sihag S, Cresci S, Li AY, Sucharov CC, and Lehman JJ. PGC-1alpha and ERRalpha target gene downregulation is a signature of the failing human heart. *J Mol Cell Cardiol.* 2009;46(2):201-12.

57. Arany Z, Novikov M, Chin S, Ma Y, Rosenzweig A, and Spiegelman BM. Transverse aortic constriction leads to accelerated heart failure in mice lacking PPAR-gamma coactivator 1alpha. *Proc Natl Acad Sci U S A.* 2006;103(26):10086-91.

58. Lai L, Leone TC, Zechner C, Schaeffer PJ, Kelly SM, Flanagan DP, Medeiros DM, Kovacs A, and Kelly DP. Transcriptional coactivators PGC-1alpha and PGC-lbeta control overlapping programs required for perinatal maturation of the heart. *Genes Dev.* 2008;22(14):1948-61.

59. Fukushima A, Alrob OA, Zhang L, Wagg CS, Altamimi T, Rawat S, Rebeyka IM, Kantor PF, and Lopaschuk GD. Acetylation and succinylation contribute to maturational alterations in energy metabolism in the newborn heart. *Am J Physiol Heart Circ Physiol.* 2016;311(2):H347-63.

60. Matsushima S, and Sadoshima J. The role of sirtuins in cardiac disease. *Am J Physiol Heart Circ Physiol.* 2015;309(9):H1375-89.

61. Hsu YJ, Hsu SC, Hsu CP, Chen YH, Chang YL, Sadoshima J, Huang SM, Tsai CS, and Lin CY. Sirtuin 1 protects the aging heart from contractile dysfunction mediated through the inhibition of endoplasmic reticulum stress-mediated apoptosis in cardiac-specific Sirtuin 1 knockout mouse model. *International journal of cardiology.* 2017;228(543-52.

62. Baur JA, and Sinclair DA. Therapeutic potential of resveratrol: the in vivo evidence. *Nat Rev Drug Discov.* 2006;5(6):493-506.

63. Lagouge M, Argmann C, Gerhart-Hines Z, Meziane H, Lerin C, Daussin F, Messadeq N, Milne J, Lambert P, Elliott P, et al. Resveratrol improves mitochondrial function and protects against metabolic disease by activating SIRT1 and PGC-1alpha. *Cell.* 2006;127(6):1109-22.

64. Dolinsky VW, and Dyck JR. Experimental studies of the molecular pathways regulated by exercise and resveratrol in heart, skeletal muscle and the vasculature. *Molecules.* 2014;19(9):14919-47.

65. Winnik S, Auwerx J, Sinclair DA, and Matter CM. Protective effects of sirtuins in cardiovascular diseases: from bench to bedside. *Eur Heart J.* 2015;36(48):3404-12.

66. Beaudoin MS, Perry CG, Arkell AM, Chabowski A, Simpson JA, Wright DC, and Holloway GP. Impairments in mitochondrial palmitoyl-CoA respiratory kinetics that precede development of diabetic cardiomyopathy are prevented by resveratrol in ZDF rats. *J Physiol.* 2014;592(12):2519-33.

67. Cao MM, Lu X, Liu GD, Su Y, Li YB, and Zhou J. Resveratrol attenuates type 2 diabetes mellitus by mediating mitochondrial biogenesis and lipid metabolism via Sirtuin type 1. *Experimental and therapeutic medicine.* 2018;15(1):576-84.

68. Fang WJ, Wang CJ, He Y, Zhou YL, Peng XD, and Liu SK. Resveratrol alleviates diabetic cardiomyopathy in rats by improving mitochondrial function through PGC-1alpha deacetylation. *Acta Pharmacol Sin.* 2017.

69. Dominy JE, Jr., Lee Y, Jedrychowski MP, Chim H, Jurczak MJ, Camporez JP, Ruan HB, Feldman J, Pierce K, Mostoslavsky R, et al. The deacetylase Sirt6 activates the acetyltransferase GCN5 and suppresses hepatic gluconeogenesis. *Molecular cell.* 2012;48(6):900-13.

70. Lu JQ. Traditional Chinese medical theory and human circadian rhythm in the occurrence of ischemic stroke. *Stroke.* 1991;22(10):1329.

71. Caton PW, Nayuni NK, Kieswich J, Khan NQ, Yaqoob MM, and Corder R. Metformin suppresses hepatic gluconeogenesis through induction of SIRT1 and GCN5. *The Journal of endocrinology.* 2010;205(1):97-106.

72. Milne JC, Lambert PD, Schenk S, Carney DP, Smith JJ, Gagne DJ, Jin L, Boss O, Perni RB, Vu CB, et al. Small molecule activators of SIRT1 as therapeutics for the treatment of type 2 diabetes. *Nature.* 2007;450(7170):712-6.

73. Lerin C, Rodgers JT, Kalume DE, Kim SH, Pandey A, and Puigserver P. GCN5 acetyltransferase complex controls glucose metabolism through transcriptional repression of PGC-1alpha. *Cell Metab.* 2006;3(6):429-38.

74. Dash S, Xiao C, Morgantini C, Szeto L, and Lewis GF. High-dose resveratrol treatment for 2 weeks inhibits intestinal and hepatic lipoprotein production in overweight/obese men. *Arterioscler Thromb Vasc Biol.* 2013;33(12):2895-901.

75. Hsu CP, Zhai P, Yamamoto T, Maejima Y, Matsushima S, Hariharan N, Shao D, Takagi H, Oka S, and Sadoshima J. Silent information regulator 1 protects the heart from ischemia/reperfusion. *Circulation.* 2010;122(21):2170-82.

76. Hoffman M, Kyriazis ID, Lucchese AM, de Lucia C, Piedepalumbo M, Bauer M, Schulze PC, Bonios MJ, Koch WJ, and Drosatos K. Myocardial Strain and Cardiac Output are Preferable Measurements for Cardiac Dysfunction and Can Predict Mortality in Septic Mice. *Journal of the American Heart Association.* 2019;8(10):e012260.

77. Bosma M, Dapito DH, Drosatos-Tampakaki Z, Huiping-Son N, Huang LS, Kersten S, Drosatos K, and Goldberg IJ. Sequestration of fatty acids in triglycerides prevents endoplasmic reticulum stress in an in vitro model of cardiomyocyte lipotoxicity. *Biochim Biophys Acta.* 2014;1841(12):1648-55.

78. Kokkinaki D, Hoffman M, Kalliora C, Kyriazis ID, Maning J, Lucchese AM, Shanmughapriya S, Tomar D, Park JY, Wang H, et al. Chemically synthesized Secoisolariciresinol diglucoside (LGM2605) improves mitochondrial function in cardiac

myocytes and alleviates septic cardiomyopathy. *Journal of molecular and cellular cardiology.* 2019;127(232-45.

FIGURES

Figure 1.

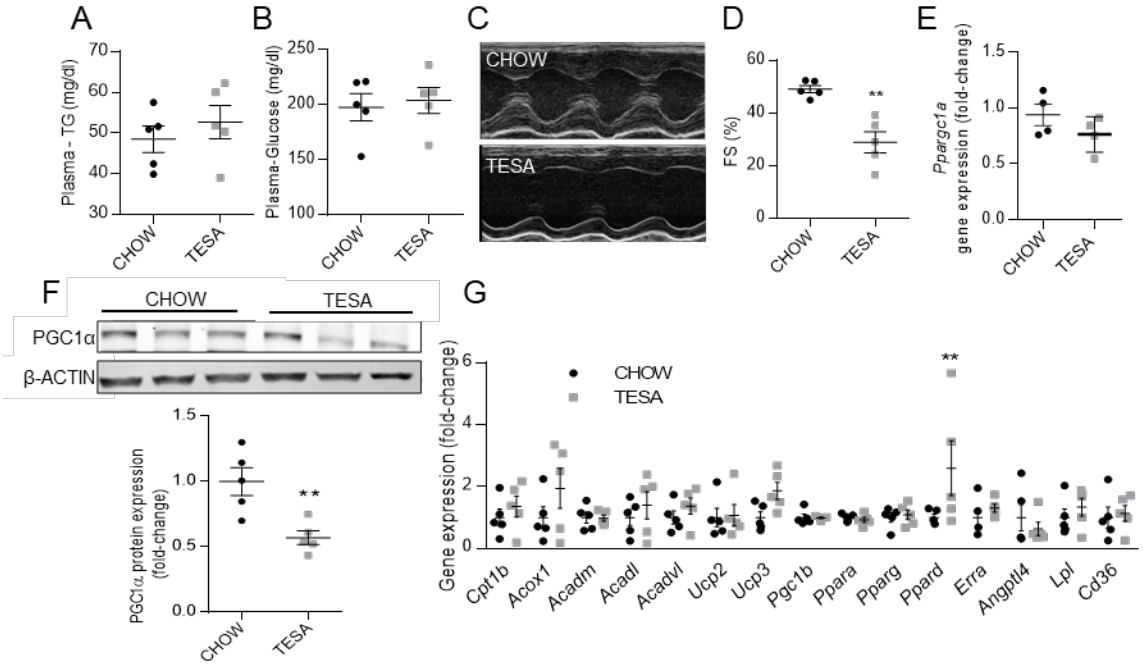

Figure 1: Tesaglitazar (TESA) causes cardiac dysfunction – A-G: C57BL/6 mice were treated with control chow or tesaglitazar-containing chow (0.5µmol/kg bw) for 6 weeks (all mice were treated in one experiment). After termination of treatment, plasma triglycerides (TG, A; n=5), plasma glucose (B; n=5) were assessed. Cardiac function was determined and represented here with short-axis M-mode echocardiography images (C) and calculation of left ventricular fractional shortening (D; n=5). After treatment period, cardiac peroxisome proliferative activated receptor gamma coactivator 1 alpha (*PPARGC1a*) mRNA levels (E; n=4) and the respective protein levels (PGC1α) were assessed (F; representative immunoblot and densitometric analysis normalized to β-ACTIN; n=5). **G.** Cardiac carnitine palmitoyltransferase 1-beta (*CPT1b*), acyl-CoA oxidase 1 (*ACOX1*), medium-chain acyl-CoA dehydrogenase (*ACADM*), long-chain acyl-CoA dehydrogenase (*ACADL*), very long-chain acyl-CoA dehydrogenase (*ACADVL*), uncoupling protein 2 (*UCP2*), *UCP3*, bagda*PPARGC1b*, peroxisome proliferator activated receptor alpha (*PPARa*), *PPARg*, *PPARd*, estrogen-related receptor alpha (*ERRa*), angiopoietin like-4 (*ANGPTL4*), lipoprotein lipase (*LPL*), and cluster of differentiation 36 (*CD36*) mRNA levels were

assessed (G; n=5). Statistical analysis was performed using unpaired 2-tailed Student's t-test. *p<0.05, **p<0.01, ***p<0.001. Error bars represent SEM.

Figure 2.

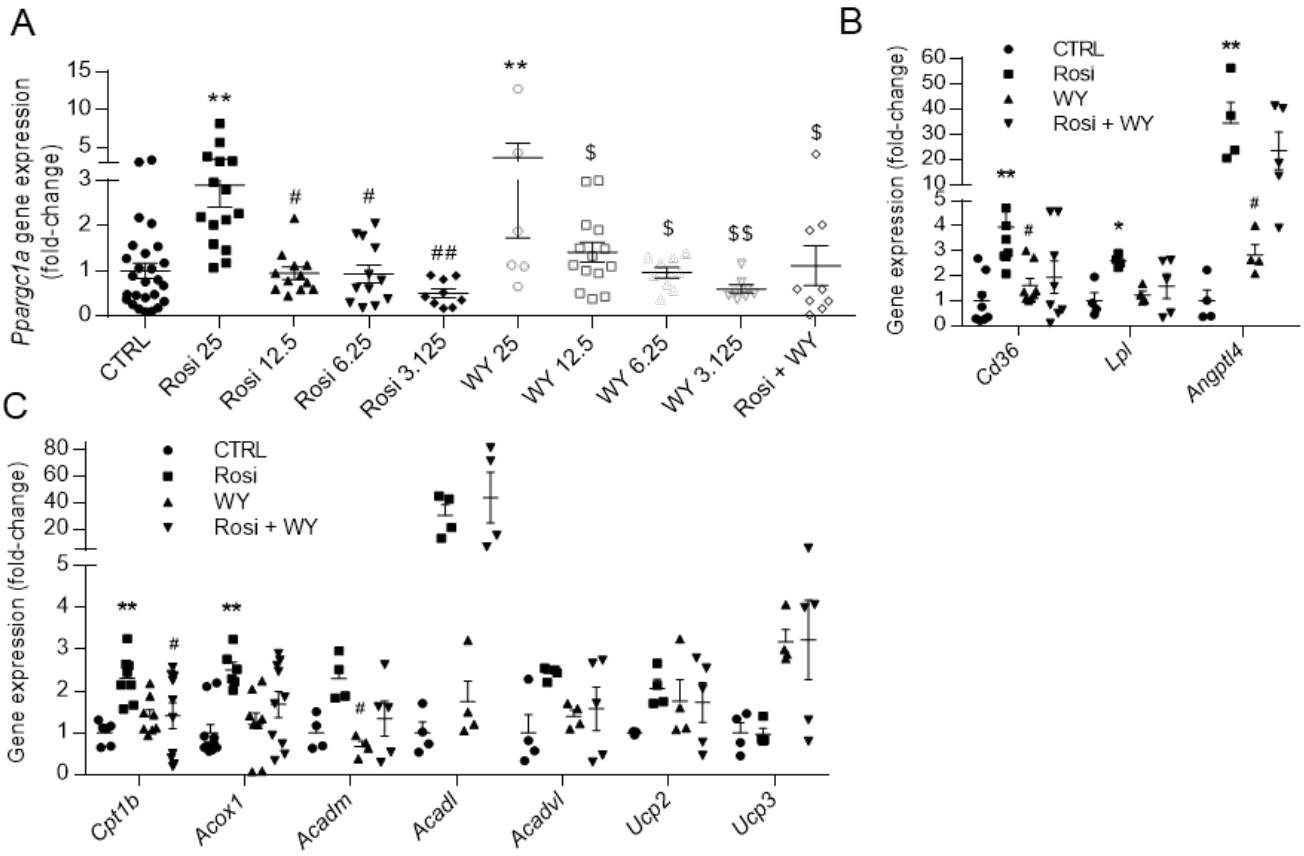

Figure 2: Peroxisome proliferator-activated receptor-alpha (PPARα) interferes with PPARγ-mediated induction of tesaglitazar on peroxisome proliferator-activated receptor gamma coactivator 1-alpha (*Ppargc1a*) expression. **A***a*: C57BL/6 mice injected intraperitoneally with 25, 12.5, 6.25, and 3.125mg/kg of body weight (bw) rosiglitazone (PPARγ agonist), and 3.125mg/kg bw WY-14643 (PPARα agonist) or combination of rosiglitazone (25mg/kg bw) and WY-14643 (12.5mg/kg bw) to assess the cardiac *PPARGC1a* mRNA levels (n=6-16). Control (CTRL) mice (n=26) received DMSO. **B-C:** C57BL/6 mice were treated intraperitoneally with rosiglitazone (25mg/kg bw), WY-14643 (12.5mg/kg bw), or combination of rosiglitazone (25mg/kg body weight) and WY-14643 (12.5mg/kg bw) and cardiac cluster of differentiation (*CD36*), lipoprotein lipase (*LPL*), angiopoietin like-4 (*ANGPTL4*) (B; n=4-8), carnitine palmitoyltransferase 1-beta (*CPT1b*), acyl-CoA oxidase 1 (*ACOX1*), medium-chain acyl-CoA dehydrogenase (*ACADM*), long-chain acyl-CoA dehydrogenase (*ACADL*), very long-chain acyl-CoA dehydrogenase (*ACADVL*), uncoupling protein 2 (*UCP2*), and *UCP3* (C; n=4-10) mRNA levels

were assessed. Control mice were treated with DMSO. Statistical analyses were performed with 1-way ANOVA followed by Tukey correction. Error bars represent SEM. *p<0.05 vs CTRL, **p<0.01 vs CTRL. $^{\#}$p<0.05 vs rosiglitasone (25mg/kg bw). $^{\#\#}$p<0.01 vs rosiglitasone (25mg/kg bw). $^{\$}$p<0.05 vs WY-14643 (25mg/kg bw). $^{\$\$}$p<0.05 vs WY-14643 (25mg/kg bw). The data presented here was collected from 2-3 independent experiments.

Figure 3.

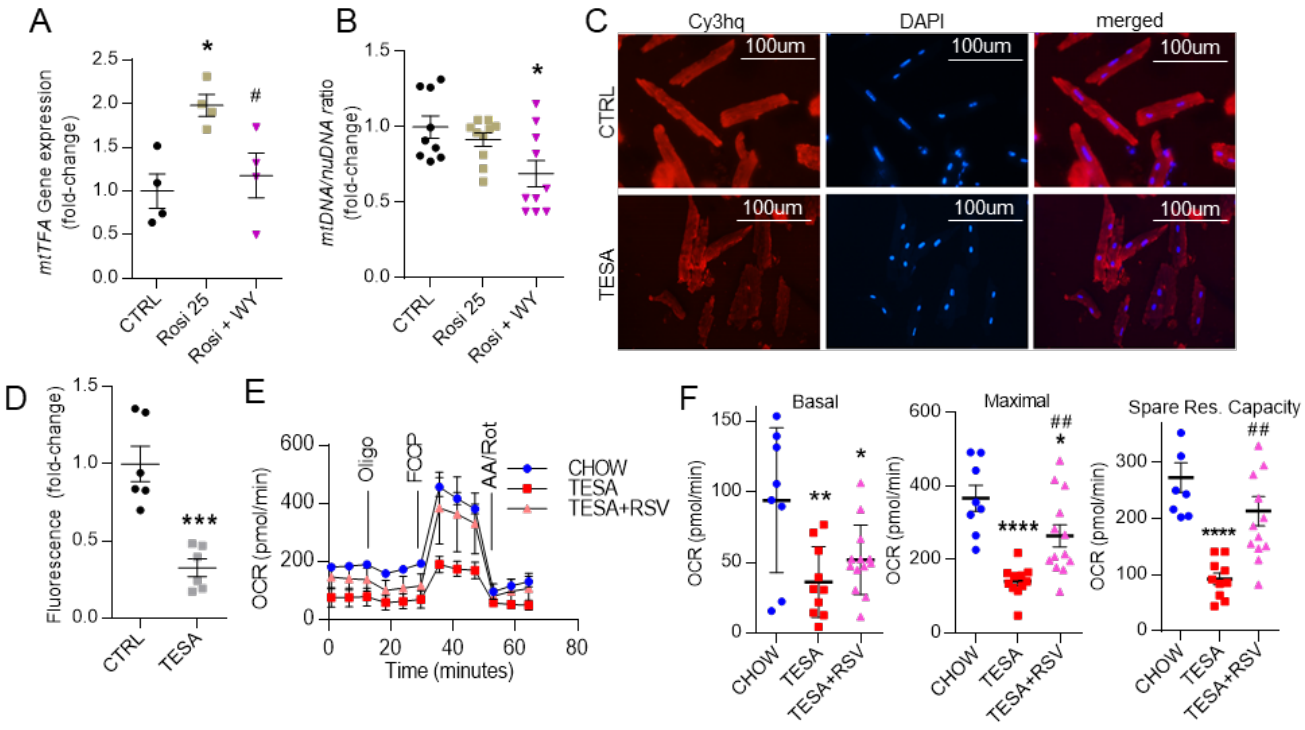

Figure 3: Tesaglitazar (TESA) reduces mitochondrial abundance in cardiomyocytes. A-B: C57BL/6 mice were injected intraperitoneally with rosiglitazone (PPARγ agonist; 25mg/kg bw), WY-14643 (PPARα agonist; 12.5mg/kg bw) or combination of rosiglitazone (25mg/kg bw) and WY-14643 (12.5mg/kg bw). Cardiac mitochondrial transcription factor A (*TFAM*) mRNA levels (A; n=4) and mitochondrial abundance was determined by measuring mitochondrial (mt)DNA to nuclear (nu)DNA ratio (fold-change) (B; n=9-10). Control (CTRL) mice were treated with DMSO. **C-D:** C57BL/6 mice were subjected to daily intraperitoneal injections with tesaglitazar (2mg/kg bw) for 7 days and primary adult cardiomyocytes (ACMs) were isolated. Representative images (C; magnification x20) obtained from fluorescence microscopy of isolated ACMs stained with MitoTracker Red and mitochondrial number/total area was quantified (D) (n=6, number of analyzed cells: control (CTRL):127, tesaglitazar:125 – Data derived from three independent experiments). **E-F.** ACMs were isolated from C57BL/6 mice upon completion of 6 weeks feeding on regular chow, chow diet containing tesaglitazar (0.5umol/kg body weight) or chow with combination of tesaglitazar (0.5umol/kg body weight) and resveratrol (RSV; 100mg/kg body

weight/day). Oxygen consumption rate (OCR; E), basal respiration, maximal respiration, and spare respiratory capacity (F) measured with XF96 Seahorse Analyzer Oligo denotes oligomycin (3μM), FCCP denotes carbonyl cyanide-p-trifluoromethoxyphenylhydrazone (2μM), AA/Rot denotes antimycin a/rotenone (0.5μM) (n=8-13 wells with ACMs isolated from three individual mice per experimental group). Statistical analyses for all graphs were performed with 1-way ANOVA followed by Tukey correction except D which was analyzed with an unpaired 2-tailed Student's t-test. *p<0.05, **p<0.01, ***p<0.001, ****p<0.0001 vs CTRL or chow. $^{\#}$p<0.05, $^{\#\#}$p<0.01 vs rosiglitazar 25 or tesaglitazar. Error bars represent SEM. * indicates statistical difference with ctrl-chow, # indicates difference with rosiglitazone or tesaglitazar treated mice.

Figure 4.

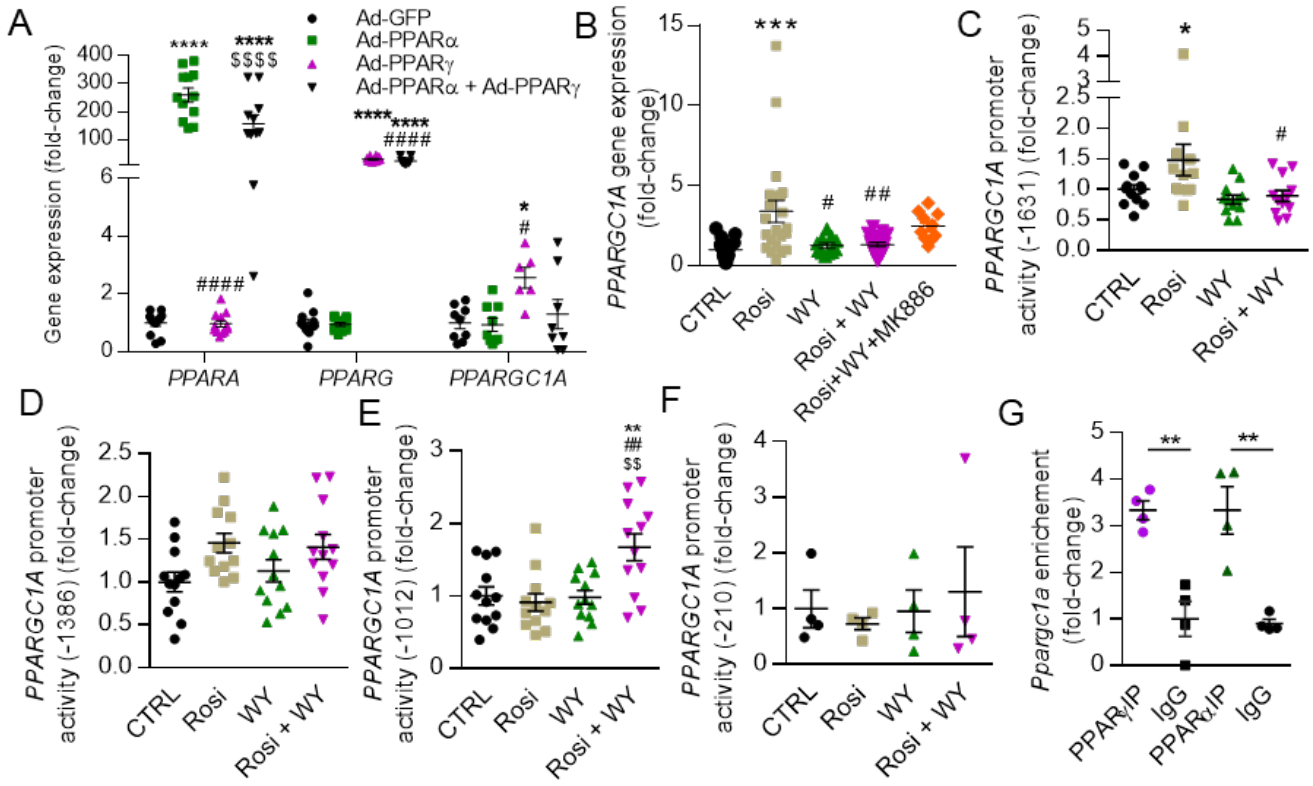

Figure 4: Peroxisome proliferator-activated receptor alpha (PPARα) impairs PPARγ-mediated activation of peroxisome proliferator-activated receptor gamma coactivator 1-alpha (*PPARGC1A*) promoter activity. A: *PPARA*, *PPARG* and *PPARGC1A* mRNA levels were assessed in AC16 cells infected with recombinant adenoviruses (Ad) expressing PPARα or PPARγ (n=6-12; data was collected from two independent experiments). *p<0.05, ****p<0.0001 vs Ad-GFP, $^{\#}$p<0.05, $^{\#\#\#\#}$p<0.0001 vs Ad-PPARα, $^{\$\$\$\$}$p<0.0001 vs Ad-PPARγ. **B:** *PPARGC1A* mRNA levels in AC16 cells treated with 50μM rosiglitazone (PPARγ agonist), 50μM WY-14643 (PPARα agonist), combination of rosiglitazone and WY-14643, or combination of rosiglitazone, WY-14643, and 10μM MK886 (PPARα antagonist) (B; n=10-22; data was collected from two independent experiments). **C-F:** Luciferase activity (fold-change) in AC16 cells transfected with reporter plasmids containing the following human *PPARGC1A* promoter fragments: pGL3-basic vector(BV)-*PPARGC1A*-1631 (C), pGL3BV-a-*PPARGC1A*-1386 (D), pGL3BV-a-*PPARGC1A*-1012 (E), pGL3BV-a-*PPARGC1A*-210 (F) followed by treatment with 50μM rosiglitazone, 50μM

WY-14643 or combination of both (n=4-12). (B-F; data was collected from one experiment, *p<0.05, **p<0.01, ***p<0.001 vs ctrl, $^{\#}$p<0.05, $^{\#\#}$p<0.01 vs rosiglitazone, $^{\$\$}$p<0.01 vs WY-14642) **G:** PPARα and PPARγ enrichment of the *Ppargc1a* gene promoter following chromatin immunoprecipitation from cardiac tissue obtained from C57BL/6 mice (n=4). Statistical analyses were performed with 1-way ANOVA followed by Tukey post-hoc correction. **p<0.01. Error bars represent SEM.

Figure 5.

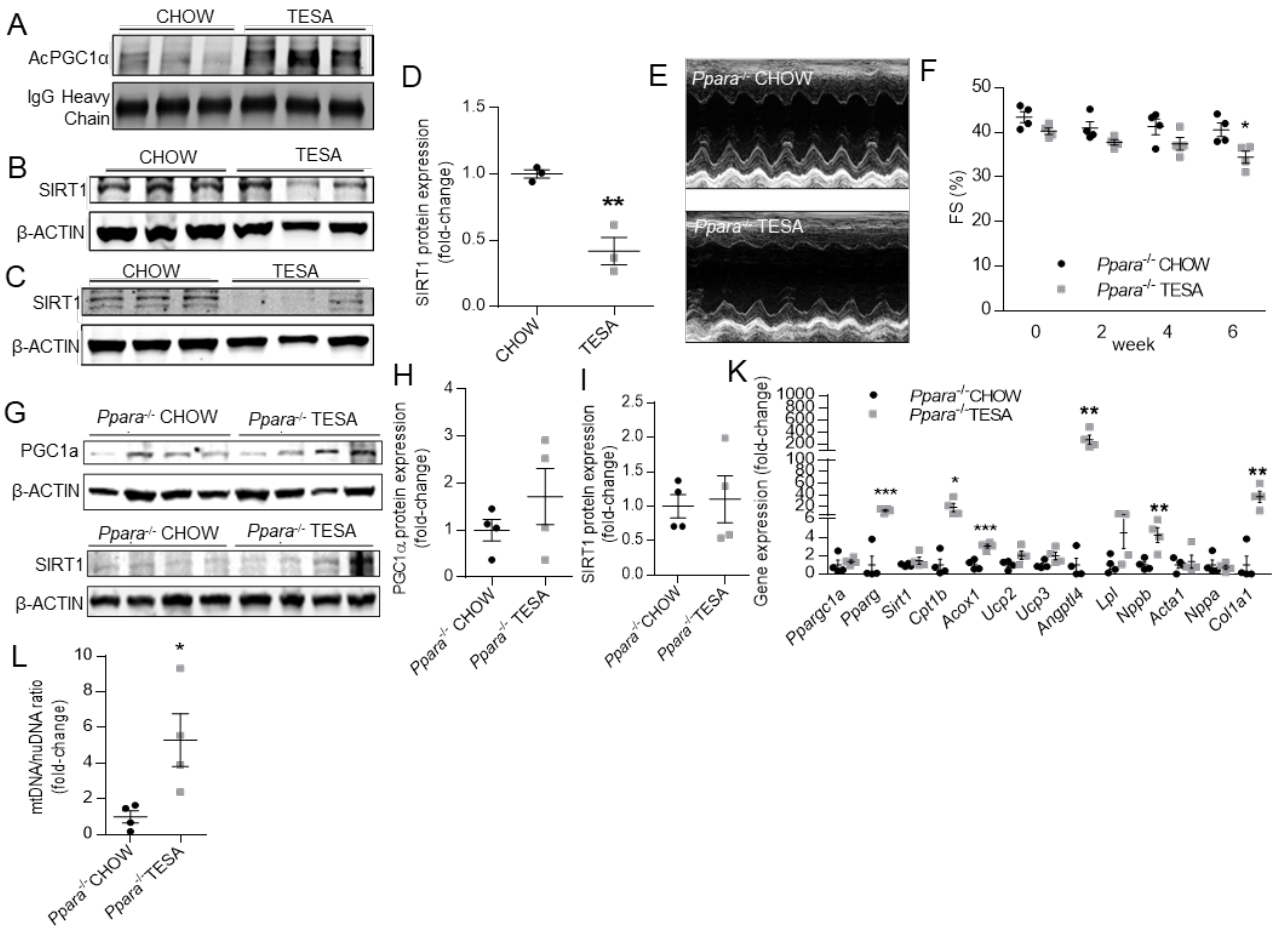

Figure 5: Tesaglitazar suppresses sirtuin1 (SIRT1) expression and promotes acetylation of peroxisome proliferator-activated receptor gamma coactivator 1-alpha (PGC1α) – A, B: Immunoblot of anti-PGC1α following immunoprecipitation with anti-Ac-Lysine antibody of acetylated-PGC1α (Ac-PGC1α) and of the heavy IgG chain (A), SIRT1 and β-ACTIN protein levels (B) in hearts obtained from C57BL/6 mice fed on regular or tesaglitazar-containing chow (0.5μmol/kg bw) diet for 6 weeks (densitometric analysis is shown in Figures S5A, B and statistical analysis was performed for data collected from 2 independent experiments; n=8). **C, D:** Representative immunoblot and densitometric analysis of SIRT1 and β-ACTIN protein levels in ACMs isolated from C57BL/6 mice treated intraperitoneally with tesaglitazar (2mg/kg bw) for 7 days (n=3; all data was collected from one experiment). **E, F**: Mice that are knockout for peroxisome proliferator-activated receptor alpha **(***Ppara)*$^{-/-}$ were fed with regular or tesaglitazar-

containing chow (0.5µmol/kg bw) diet for 6 weeks (n=4, all data was collected from one experiment). Representative short-axis M-mode echocardiography images (E) and left ventricular fractional shortening (F) of *Ppara*$^{-/-}$ mice treated with regular or tesaglitazar-containing chow for 6 weeks. **G-L**: Representative immunoblots (F) and densitometric analysis of PGC1α (G, H), SIRT1 (G, I) and β-ACTIN protein levels, cardiac *PPARGC1a*, *PPARg*, *SIRT1*, bcarnitine palmitoyltransferase 1-beta (*CPT1b*), acyl-CoA oxidase 1 (*ACOX1*), uncoupling protein 2 (*UCP2*), *UCP3*, angiopoietin like-4 (*ANGPTL4*), lipoprotein lipase (*LPL*), natriuretic peptide B (*NPPB*), actin alpha 1 (*ACTA1*), natriuretic peptide type A (*NPPA*) and collagen type I alpha 1 chain (*COL1A1*) mRNA levels (J), and mitochondrial (mt)DNA to nuclear (nu)DNA ratio (K) in hearts obtained from *Ppara*$^{-/-}$ mice fed on regular or tesaglitazar-containing chow (0.5µmol/kg bw) for 6 weeks (n=4). Statistical analyses were performed with unpaired 2-tailed Student's t-tests, *p<0.05, **p<0.01, ***p<0.001 vs chow. Error bars represent SEM.

Figure 6.

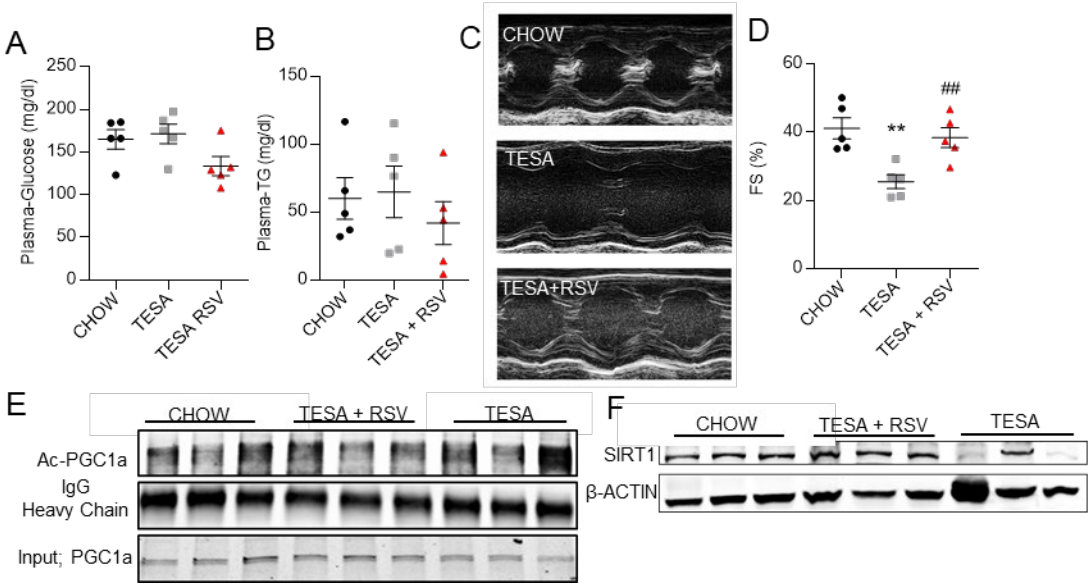

Figure 6: Resveratrol (RSV) negates the cardiotoxic effect of tesaglitazar. A-D: C57BL/6 mice were fed on chow containing tesaglitazar (0.5μmol/kg bw), combination of tesaglitazar (0.5μmol/kg bw) and resveratrol (RSV; 100mg/kg bw/day) or regular chow for 6 weeks. Plasma glucose (A), plasma triglycerides (TG) (B) were determined upon completion of the treatment. Representative short-axis M-mode echocardiography images (C; after treatment termination) and left ventricular fractional shortening (D) of C57BL/6 mice fed on chow containing tesaglitazar (0.5μmol/kg bw) or combination of tesaglitazar (0.5μmol/kg bw) and RSV (100mg/kg bw/day) for 6 weeks (n=5; data was collected from one experiment). **E, F**: Immunoblots of cardiac acetylated-peroxisome proliferator activated receptor gamma coactivator 1-alpha (ac-PGC1α) (E), IgG heavy chain, total PGC1α, sirtuin1 (SIRT1), and β-ACTIN (F) of C57BL/6 mice fed on regular chow or chow containing tesaglitazar (0.5μmol/kg bw) or combination of tesaglitazar (0.5μmol/kg bw) and RSV (100mg/kg bw/day) for 6 weeks (densitometric analysis is shown in Figures S5A, B and statistical analysis was performed for data collected from 2 independent experiments; n=5-8). Statistical analyses were performed with 1-way ANOVA followed by Tukey post-hoc correction among groups. **p<0.01 vs chow, ##p<0.01 vs tesaglitazar. Error bars represent SEM.

Figure 7.

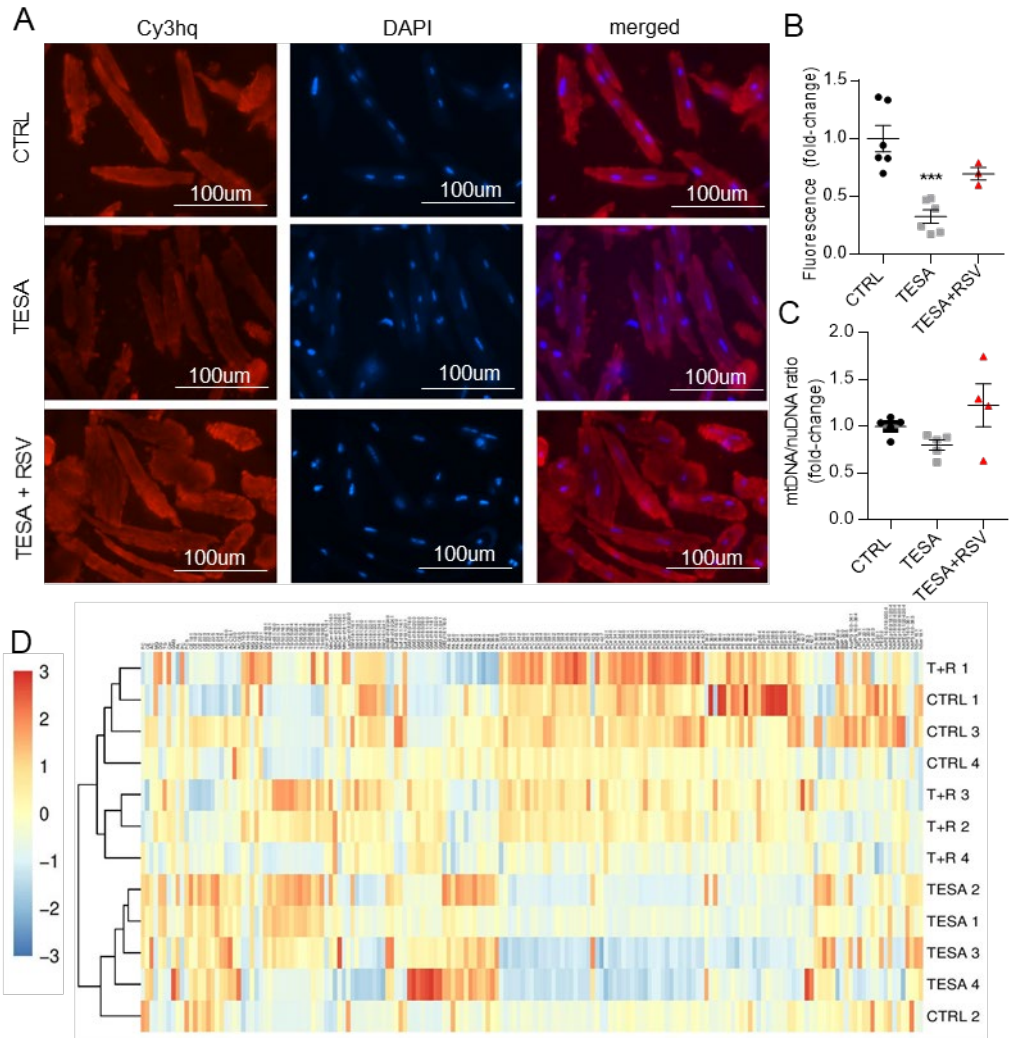

Figure 7: Resveratrol (RSV) restores mitochondrial function, abundance and lipid homeostasis in mice treated with tesaglitazar - A, B: Adult cardiomyocytes (ACMs) were obtained from C57BL/6 mice that were subjected to intraperitoneal daily injections of tesaglitazar (TESA; 2mg/kg bw) or combination of tesaglitazar (2mg/kg bw) and RSV (100mg/kg bw) for 7 days. Representative fluorescence microscopy images (A; magnification x20) of isolated ACMs stained with MitoTracker Red and quantitation (B) of mitochondrial number/total area (number of analyzed cells: 158 cells from 6 control (CTRL) mice; 157 cells from 6 tesaglitazar (TESA)-fed mice; 157 cells from 3 mice treated with tesaglitazar and resveratrol (TESA+RSV). All treatments were performed in one experiment. **C**: Cardiac mitochondrial (mt)DNA to nuclear (nu)DNA ratio (fold-change) in C57BL/6 mice fed with chow diet containing tesaglitazar (0.5µmol/kg bw) or

combination of tesaglitazar (0.5μmol/kg bw) and resveratrol (100mg/kg bw/day) for 6 weeks, (n=4-5)**. D:** Heat map and correlation clustering following lipidomic analysis of hearts obtained from C57BL/6 mice fed with chow diet containing tesaglitazar or combination of tesaglitazar and resveratrol for 6 weeks (n=4). Statistical analyses were performed with 1-way ANOVA followed by Tukey post-hoc correction among groups. ***p<0.001 vs chow. Error bars represent SEM.

Figure 8.

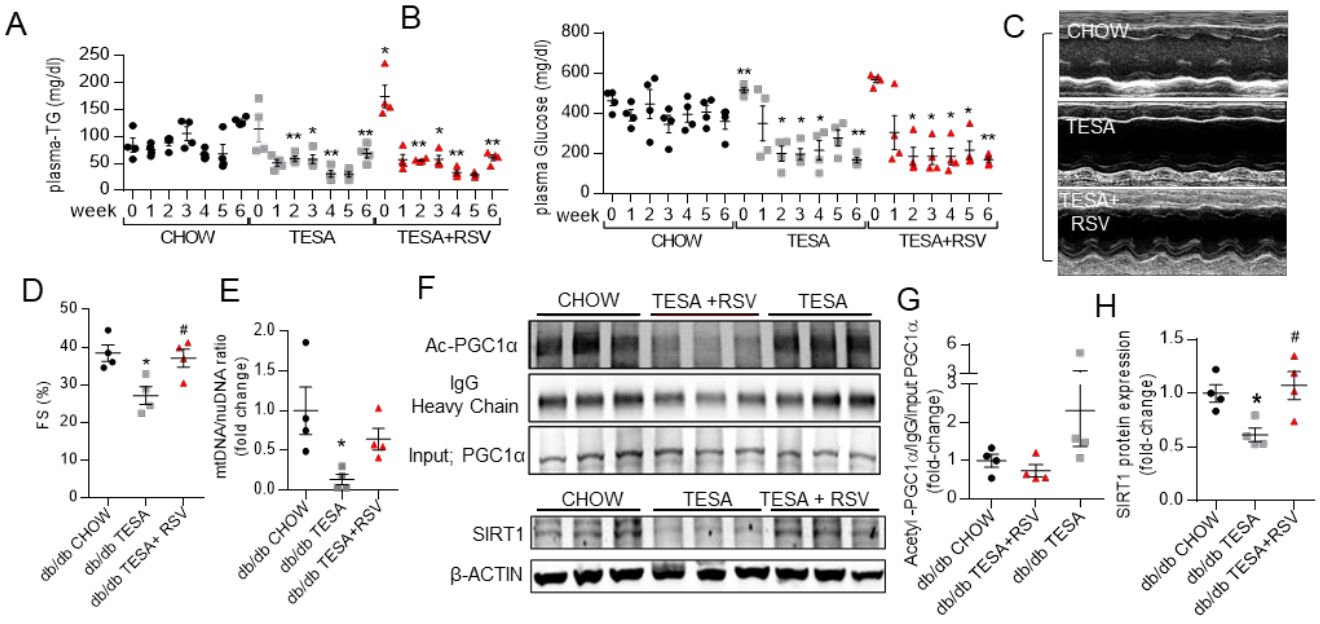

Figure 8: Resveratrol (RSV) blocks the cardiotoxic effect of tesaglitazar in diabetic mice -

A-H: Leptin-receptor-deficient (*db/db*) mice were treated with regular chow or chow containing either tesaglitazar (TESA; 0.5μmol/kg bw) or combination of tesaglitazar (0.5μmol/kg bw) and RSV (100mg/kg bw/day) for 6 weeks. Plasma triglycerides (TG) (A), plasma glucose (B) were determined throughout the treatment. Representative short-axis M-mode images (C), left ventricular fractional shortening (D), and mitochondrial (mt)DNA to nuclear (nu)DNA ratio (fold-change) (E) were determined upon termination of the treatment (n=4; data was collected from one experiment). Cardiac acetylated peroxisome proliferator-activated receptor gamma coactivator 1-alpha (Ac-PGC1α) normalized to IgG heavy chain, and total PGC1α, sirtuin1 (SIRT1), β-ACTIN immunoblots (F) and densitometric analysis (G, H) of *db/db* mice fed on regular chow, tesaglitazar-containing chow or chow that contains tesaglitazar and resveratrol diet for 6 weeks (n=4; data was collected from one experiment). (n=4). Statistical analysis was performed with 1-way ANOVA followed by Tukey post-hoc correction. *p<0.05, **p<0.01 vs chow #p<0.05 vs tesaglitazar. Error bars represent SEM.

Figure 9.

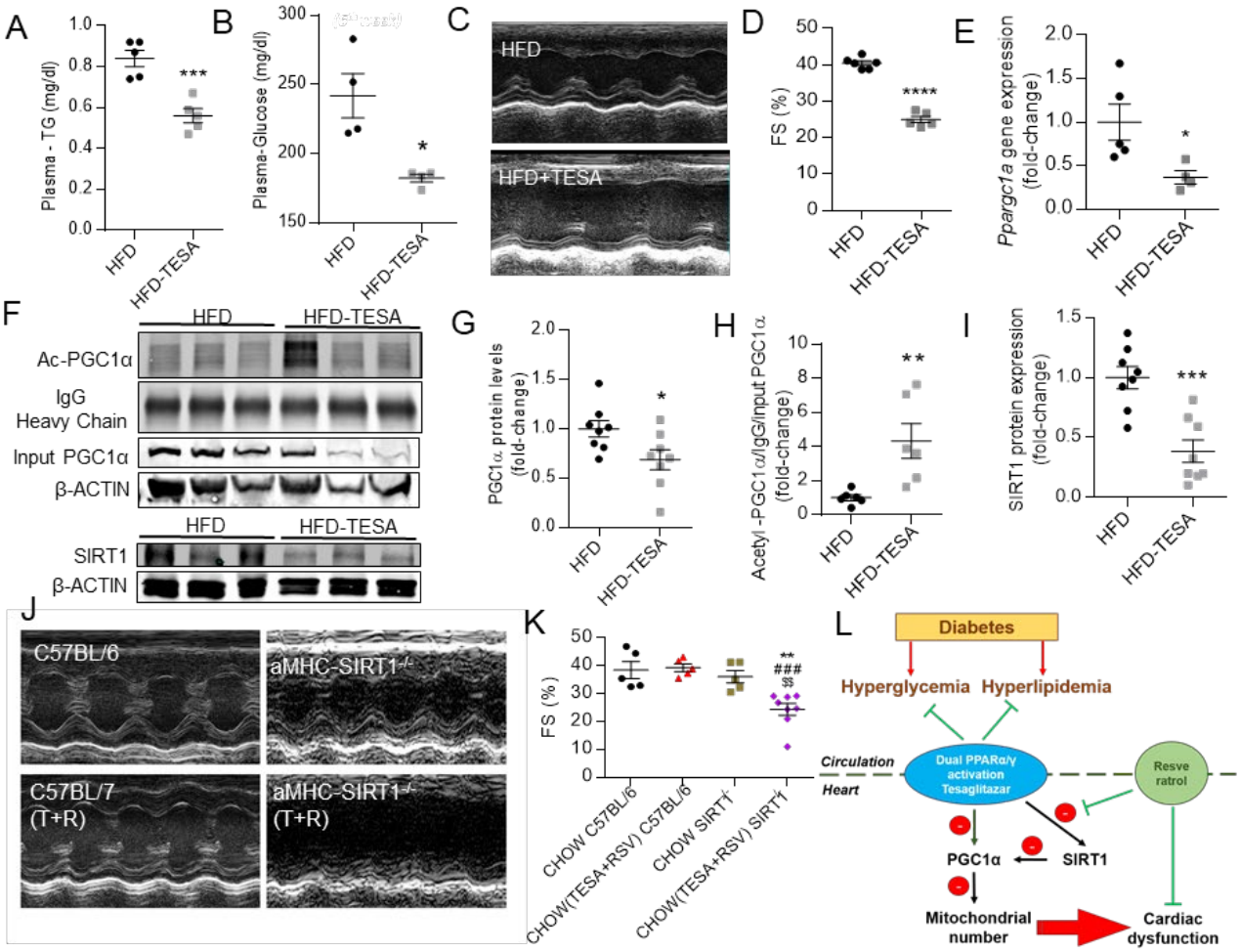

Figure 9: Cardiac SIRT1 ablation abrogates resveratrol (RSV) beneficial effect in tesaglitazar-mediated cardiac dysfunction. A-H: C57BL/6 mice fed with high fat diet (HFD) or HFD containing tesaglitazar (0.5μmol/kg bw) for 6 weeks (all data was collected from one experiment). Upon completion of the treatment, plasma triglycerides (TG; A) and glucose levels (B) were determined. Representative short-axis M-mode images (C) and left ventricular fractional shortening (D) of C57BL/6 mice fed on regular or tesaglitazar-containing HFD for 6 weeks (n=5-6). Cardiac peroxisome proliferator-activated receptor gamma coactivator 1-alpha (*Ppargc1a*) *(*E; n=4-5) gene expression, acetylated peroxisome proliferator-activated receptor gamma coactivator 1-alpha (Ac-PGC1α; n=6) normalized to IgG heavy chain and total PGC1α (n=8), sirtuin1 (SIRT1; n=8), β-ACTIN immunoblots (F) and their densitometric analysis (G-I) from

C57BL/6 mice treated on regular or tesaglitazar- containing HFD (0.5μmol/kg bw). **J, K:** Representative short-axis M-mode images (J) and left ventricular fractional shortening (%) (K) of C57BL/6 mice and alpha myosin heavy chain-(aMHC)-*Sirt1*$^{-/-}$ mice fed on regular chow or chow containing combination of tesaglitazar (0.5μmol/kg bw) and resveratrol (RSV; 100mg/kg bw/day) (n=5-8; data was collected from two independent experiments). Statistical analysis for graphs A-I was performed with unpaired 2-tailed Student's t-tests. Statistical analysis for graph K was performed with 1-way ANOVA followed by Tukey post-hoc correction. *p<0.05, **p<0.01, ***p<0.001, ****p<0.0001 vs HFD (A-I) or chow C57BL6 (K). $^{###}$p<0.001 vs tesaglitazar plus RSV C57BL/6. $^{\$\$}$p<0.01 vs chow aMHC-*Sirt1*$^{-/-}$. Error bars represent SEM. **L. Schematic representation of the proposed model** - Tesaglitazar treats hyperlipidemia and hyperglycemia but suppresses SIRT1 and PGC1α, which reduces mitochondrial abundance and causes cardiac dysfunction. The aggravating effect of tesaglitazar on cardiac function is alleviated by co-administration of RSV.